











TECH BRIEFS

NATIONAL AERONAUTICS AND SPACE ADMINISTRATION

-  **Technology Focus**
-  **Electronics/Computers**
-  **Software**
-  **Materials**
-  **Mechanics/Machinery**
-  **Manufacturing**
-  **Bio-Medical**
-  **Physical Sciences**
-  **Information Sciences**
-  **Books and Reports**

INTRODUCTION

Tech Briefs are short announcements of innovations originating from research and development activities of the National Aeronautics and Space Administration. They emphasize information considered likely to be transferable across industrial, regional, or disciplinary lines and are issued to encourage commercial application.

Additional Information on NASA Tech Briefs and TSPs

Additional information announced herein may be obtained from the NASA Technical Reports Server: <http://ntrs.nasa.gov>.

Please reference the control numbers appearing at the end of each Tech Brief. Information on NASA's Innovative Partnerships Program (IPP), its documents, and services is available on the World Wide Web at <http://www.ipp.nasa.gov>.

Innovative Partnerships Offices are located at NASA field centers to provide technology-transfer access to industrial users. Inquiries can be made by contacting NASA field centers listed below.

NASA Field Centers and Program Offices

Ames Research Center

Mary Walsh
(650) 604-1405
mary.w.walsh@nasa.gov

Dryden Flight Research Center

Ron Young
(661) 276-3741
ronald.m.young@nasa.gov

Glenn Research Center

Joe Shaw
(216) 977-7135
robert.j.shaw@nasa.gov

Goddard Space Flight Center

Nona Cheeks
(301) 286-5810
nona.k.cheeks@nasa.gov

Jet Propulsion Laboratory

Indrani Graczyk
(818) 354-2241
indrani.graczyk@jpl.nasa.gov

Johnson Space Center

John E. James
(281) 483-3809
john.e.james@nasa.gov

Kennedy Space Center

David R. Makufka
(321) 867-6227
david.r.makufka@nasa.gov

Langley Research Center

Michelle Ferebee
(757) 864-5617
michelle.t.ferebee@nasa.gov

Marshall Space Flight Center

Jim Dowdy
(256) 544-7604
jim.dowdy@nasa.gov

Stennis Space Center

Ramona Travis
(228) 688-3832
ramona.e.travis@ssc.nasa.gov

NASA Headquarters

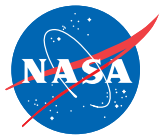
Innovative Partnerships Office

Doug Comstock, Director
(202) 358-2221
doug.comstock@nasa.gov

Daniel Lockney,
Technology Transfer Lead
(202) 358-2037
daniel.p.lockney@nasa.gov

Small Business Innovation Research (SBIR) & Small Business Technology Transfer (STTR) Programs

Carl Ray, Program Executive
(202) 358-4652
carl.g.ray@nasa.gov



TECH BRIEFS

NATIONAL AERONAUTICS AND SPACE ADMINISTRATION



5 Technology Focus: Sensors

- 5 Energy-Based Tetrahedron Sensor for High-Temperature, High-Pressure Environments
- 5 Handheld Universal Diagnostic Sensor
- 6 Large-Area Vacuum Ultraviolet Sensors
- 7 Fiber Bragg Grating Sensor System for Monitoring Smart Composite Aerospace Structures
- 7 Health-Enabled Smart Sensor Fusion Technology
- 8 Extended-Range Passive RFID and Sensor Tags
- 9 Hybrid Collaborative Learning for Classification and Clustering in Sensor Networks



11 Manufacturing & Prototyping

- 11 Self-Healing, Inflatable, Rigidizable Shelter
- 11 Improvements in Cold-Plate Fabrication



13 Electronics/Computers

- 13 Technique for Radiometer and Antenna Array Calibration — TRAAC
- 13 Real-Time Cognitive Computing Architecture for Data Fusion in a Dynamic Environment
- 14 Programmable Digital Controller
- 14 Use of CCSDS Packets Over SpaceWire to Control Hardware



17 Software

- 17 Key Decision Record Creation and Approval Module
- 17 Enhanced Graphics for Extended Scale Range
- 17 Debris Examination Using Ballistic and Radar Integrated Software
- 18 Data Distribution System (DDS) and Solar Dynamic Observatory Ground Station (SDOGS) Integration Manager
- 18 Eclipse-Free-Time Assessment Tool for IRIS
- 18 Automated and Manual Rocket Crater Measurement Software
- 18 MATLAB Stability and Control Toolbox Trim and Static Stability Module
- 18 Patched Conic Trajectory Code
- 19 Ring Image Analyzer
- 19 SureTrak Probability of Impact Display



21 Mechanics/Machinery

- 21 Implementation of a Non-Metallic Barrier in an Electric Motor
- 21 Multi-Mission Radioisotope Thermoelectric Generator Heat Exchangers for the Mars Science Laboratory Rover

- 22 Uniform Dust Distributor for Testing Radiative Emittance of Dust-Coated Surfaces
- 23 MicroProbe Small Unmanned Aerial System



25 Materials & Coatings

- 25 Highly Stable and Active Catalyst for Sabatier Reactions
- 25 Better Proton-Conducting Polymers for Fuel-Cell Membranes



27 Physical Sciences

- 27 CCD Camera Lens Interface for Real-Time Theodolite Alignment
- 27 Peregrine 100-km Sounding Rocket Project
- 28 SOFIA Closed- and Open-Door Aerodynamic Analyses
- 29 Sonic Thermometer for High-Altitude Balloons
- 29 Near-Infrared Photon-Counting Camera for High-Sensitivity Observations
- 30 Integrated Optics Achromatic Nuller for Stellar Interferometry
- 31 High-Speed Digital Interferometry
- 31 Ultra-Miniature Lidar Scanner for Launch Range Data Collection



33 Information Sciences

- 33 Shape and Color Features for Object Recognition Search
- 33 Explanation Capabilities for Behavior-Based Robot Control
- 34 A DNA-Inspired Encryption Methodology for Secure, Mobile Ad Hoc Networks



37 Bio-Medical

- 37 Quality Control Method for a Micro-Nano-Channel Microfabricated Device



39 Books & Reports

- 39 Corner-Cube Retroreflector Instrument for Advanced Lunar Laser Ranging
- 39 Electro Spray Collection of Lunar Dust
- 39 Fabrication of a Kilopixel Array of Superconducting Microcalorimeters With Microstripline Wiring
- 40 Spacecraft Attitude Tracking and Maneuver Using Combined Magnetic Actuators
- 40 Coherent Detector for Near-Angle Scattering and Polarization Characterization of Telescope Mirror Coatings

This document was prepared under the sponsorship of the National Aeronautics and Space Administration. Neither the United States Government nor any person acting on behalf of the United States Government assumes any liability resulting from the use of the information contained in this document, or warrants that such use will be free from privately owned rights.



Energy-Based Tetrahedron Sensor for High-Temperature, High-Pressure Environments

This sensor is applicable in the mining industry or in acoustic applications where energy-based measurements are required.

Stennis Space Center, Mississippi

An acoustic energy-based probe has been developed that incorporates multiple acoustic sensing elements in order to obtain the acoustic pressure and three-dimensional acoustic particle velocity. With these quantities, the user can obtain various energy-based quantities, including acoustic energy density, acoustic intensity, and acoustic impedance. In this specific development, the probe has been designed to operate in an environment characterized by high temperatures and high pressures as is found in the close vicinity of rocket plumes. Given these capabilities, the probe is designed to be used to investigate the acoustic conditions within the plume of a rocket engine or jet engine to facilitate greater understanding of the noise generation mechanisms in those plumes.

The probe features sensors mounted inside a solid sphere. The associated electronics for the probe are contained within the sphere and the associated handle for the probe. More importantly, the design of the probe has desirable properties that reduce the bias errors as-

sociated with determining the acoustic pressure and velocity using finite sum and difference techniques. The diameter of the probe dictates the lower and upper operating frequencies for the probe, where accurate measurements can be acquired. The current probe design implements a sphere diameter of 1 in. (2.5 cm), which limits the upper operating frequency to about 4.5 kHz. The sensors are operational up to much higher frequencies, and could be used to acquire pressure data at higher frequencies, but the energy-based measurements are limited to that upper frequency. Larger or smaller spherical probes could be designed to go to lower or higher frequency ranges.

The probe was manufactured using four G.R.A.S 40 BH 1/4" microphones embedded in the 1-in. (2.5-cm) sphere. The pre-amplifiers for the microphones are also embedded in the sphere. These microphones are capable of operation in sound fields up to 190 dB, which make them suitable for the rocket plume environment. The LabVIEW data

acquisition system acquires the microphone signals from each of the four probes and estimates the acoustic pressure at the center of the probe as the average of the four measured pressures. The acoustic particle velocity is obtained using finite difference techniques to acquire a velocity estimate between each pair of microphones in the tetrahedron design. These six particle velocity estimates are along different directions and estimate the particle velocity at the center point of that side of the tetrahedron. Thus, the user is required to determine the three orthogonal velocity components from these six estimates made. The advantage of using an energy-based probe is that it allows the user to extract additional information regarding the radiation characteristics of the source being investigated.

This work was done by Kent L. Gee, Scott D. Sommerfeldt, and Jonathan D. Blotter of Brigham Young University for Stennis Space Center. For more information, contact the SSC Chief Technologist Office at (228) 688-1929. Refer to SSC-00355.

Handheld Universal Diagnostic Sensor

A single drop of blood enables chemistry, hematology, and biomarker diagnostics in minutes.

John H. Glenn Research Center, Cleveland, Ohio

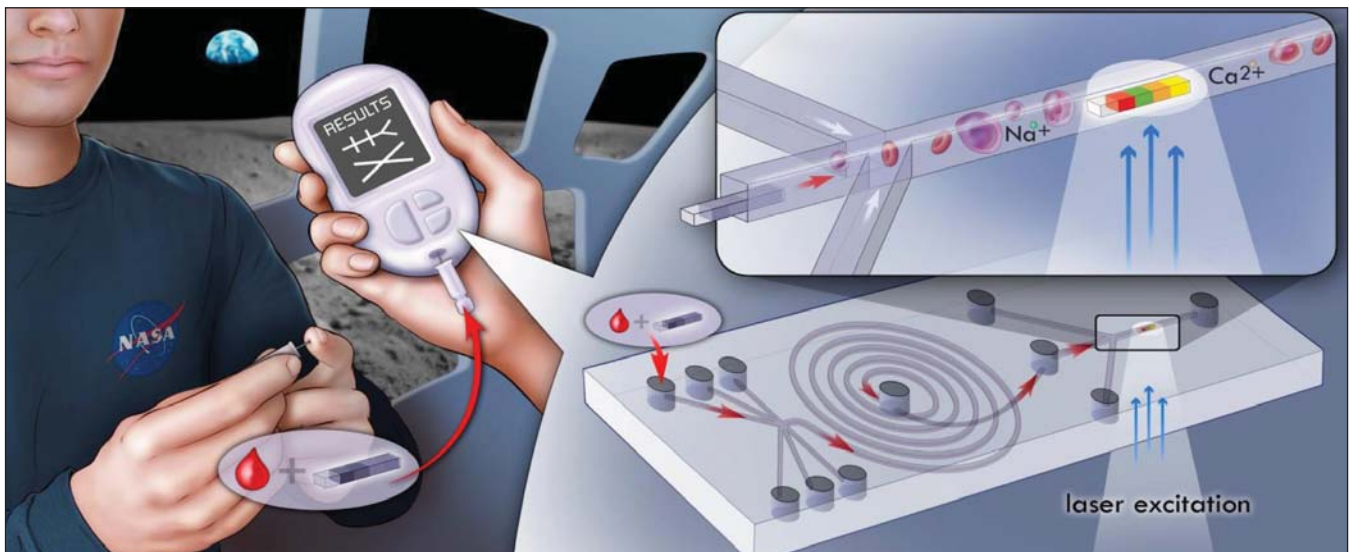
The rHEALTH technology is designed to shrink an entire hospital testing laboratory onto a handheld device. A physician or healthcare provider performs the test by collecting a fingerstick of blood from a patient. The tiny volume of blood is inserted into the rHEALTH device (see figure). Inside the device is a microfluidic chip that contains small channels about the width of a human hair. These channels help move the blood and analyze the blood sample. The rHEALTH sensor uses proprietary reagents called nanos-

trips, which are nanoscale test strips that enable the clinical assays. The readout is performed by laser-induced fluorescence. Overall, the time from blood collection through analysis is less than a minute.

The spiral-shaped microfluidic channels perform all the necessary sample preprocessing required for sample analysis. They accomplish this by mixing and diluting the blood sample in a miniaturized geometry. In contrast, for typical benchtop blood counters and clinical analyzers, these steps require au-

tomation and large amounts of reagents. Performing these steps on-chip allows these tests to be applicable for point-of-care settings. Furthermore, for reliable results, the on-chip processing steps are all compatible with the chips' flow-through geometry, which prevents blood stasis and clotting.

The rHEALTH prototype sensor is small, rugged, and fits in the palm of a hand. It uses state-of-the-art solid-state lasers and detectors that allow for robust, time-of-flight analysis of the samples. The performance remains uncompromised, al-



rHEALTH Universal Blood Sensor is designed to perform a breadth of analyses on blood or bodily fluids.

lowing high-sensitivity fluorescence analysis. Traditional flow cytometric profiles are obtained using this device. These include intensity versus intensity scatterplots and cell histograms. Flow-based, laser-induced fluorescence is thus a powerful technique that allows the user to have a universal detection platform for all of the assays, whether they be antibody, nanostrip, hematology, or biomarker assays. The microfluidic system allows a wide range of reagents, including antibodies, fluorescent

dyes, and proprietary nanoscale test strips to be mixed with the blood sample. Typical existing commercial sensors can only perform one test at a time.

The rHEALTH device employs sophisticated flow-based detection technologies that allow a wide range of samples to be counted, analyzed, and measured with a high degree of multiplexing. The sensor is able to perform a range of analyses for cells, electrolytes, biomarkers, nucleic acids, and small

molecules on a blood sample smaller than 10 μL .

This work was done by Eugene Chan of DNA Medicine Institute, Inc. for Glenn Research Center. Further information is contained in a TSP (see page 1).

Inquiries concerning rights for the commercial use of this invention should be addressed to NASA Glenn Research Center, Innovative Partnerships Office, Attn: Steven Fedor, Mail Stop 4-8, 21000 Brookpark Road, Cleveland, Ohio 44135. Refer to LEW-18727-1.

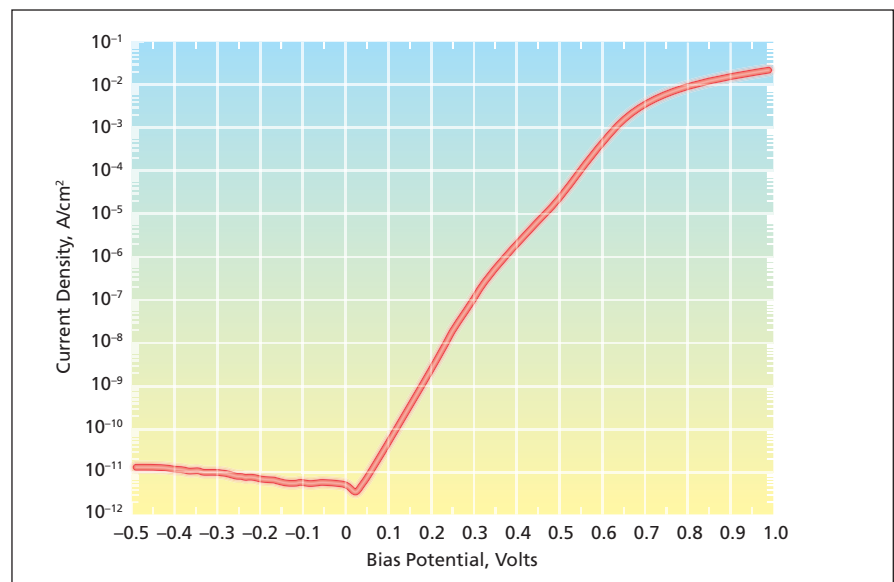
Large-Area Vacuum Ultraviolet Sensors

These devices exhibit very low dark currents.

Goddard Space Flight Center, Greenbelt, Maryland

Pt/(n-doped GaN) Schottky-barrier diodes having active areas as large as 1 cm square have been designed and fabricated as prototypes of photodetectors for the vacuum ultraviolet portion (wavelengths ≈ 200 nm) of the solar spectrum. In addition to having adequate sensitivity to photons in this wavelength range, these photodetectors are required to be insensitive to visible and infrared components of sunlight and to have relatively low levels of dark current.

In preparation for fabricating a batch of assorted prototype detectors, a c-plane (0001-plane) sapphire wafer was subjected to a rigorous cleaning by use of an acid and an organic solvent. Fabrication began with low-pressure metalorganic vapor-phase epitaxy of four GaN layers on the sapphire wafer: The first was a 25-nm-thick GaN nucleation layer. The second was a thicker GaN buffer



Current Density vs. Voltage was determined from measurements on device of the type described in the text.

layer to serve as a template for epitaxial growth. The third was a 3- μm -thick GaN epilayer containing electron-donor (n) doping at a density of $4.8 \times 10^{18} \text{ cm}^{-3}$. The fourth was a 0.75- μm -thick GaN epilayer n-doped at a density of $\approx 10^{16} \text{ cm}^{-3}$.

Four masks were used to define features of devices having Schottky contact areas ranging up to the aforementioned maximum of 1 cm square. Mesas (one for each device) were first defined by use of conventional photolithography and chlorine-bromine reactive-ion etching for complete removal of the n epilayer. Metal patterns, each consisting of a 10-nm-thick layer of Ti followed by a 10-nm-thick layer of Ni followed by a

150-nm-thick layer of Al, were defined at the bottoms of the mesas by means of a lift-off procedure and electron-beam evaporation. These metal patterns were annealed at a temperature of 500 °C for 10 minutes in flowing nitrogen to form ohmic contacts.

Next, semitransparent Pt Schottky contacts having a thickness of 10 nm were defined on the tops of the mesas by means of a lift-off procedure. Contact rings, each consisting of a 30-nm-thick layer of Pt followed by a 150-nm-thick layer of Au, were formed on the peripheries of the semitransparent Pt Schottky areas by electron-beam evaporation and lift-off.

In preliminary tests of the electrical characteristics of these devices, forward and reverse current-vs.-voltage characteristics were measured in a dark enclosure. The measurements confirmed that as desired, these devices are characterized by low levels of dark current at low reverse bias voltage: For example, one device having an active area of 0.25 cm² exhibited a leakage current density of only 14 pA/cm² at a reverse bias of 0.5 V (see figure).

This work was done by Shahid Aslam and David Franz of Raytheon Co. for Goddard Space Flight Center. Further information is contained in a TSP (see page 1). GSC-14777-1

Fiber Bragg Grating Sensor System for Monitoring Smart Composite Aerospace Structures

Dryden Flight Research Center, Edwards, California

Lightweight, electromagnetic interference (EMI) immune, fiber-optic, sensor-based structural health monitoring (SHM) will play an increasing role in aerospace structures ranging from aircraft wings to jet engine vanes. Fiber Bragg Grating (FBG) sensors for SHM include advanced signal processing, system and damage identification, and location and quantification algorithms. Potentially, the solution could be developed into an autonomous onboard system to inspect and perform non-destructive evaluation and SHM.

A novel method has been developed to massively multiplex FBG sensors, supported by a parallel processing interrogator, which enables high sampling rates combined with highly distributed sensing (up to 96 sensors per system). The interrogation system comprises several subsystems. A broadband

optical source subsystem (BOSS) and routing and interface module (RIM) send light from the interrogation system to a composite embedded FBG sensor matrix, which returns measurement-dependent wavelengths back to the interrogation system for measurement with subpicometer resolution. In particular, the returned wavelengths are channeled by the RIM to a photonic signal processing subsystem based on powerful optical chips, then passed through an optoelectronic interface to an analog post-detection electronics subsystem, digital post-detection electronics subsystem, and finally via a data interface to a computer.

A range of composite structures has been fabricated with FBGs embedded. Stress tensile, bending, and dynamic strain tests were performed. The experimental work proved that the FBG sen-

sors have a good level of accuracy in measuring the static response of the tested composite coupons (down to sub-microstrain levels), the capability to detect and monitor dynamic loads, and the ability to detect defects in composites by a variety of methods including monitoring the decay time under different dynamic loading conditions.

In addition to quasi-static and dynamic load monitoring, the system can capture acoustic emission events that can be a prelude to structural failure, as well as piezoactuator-induced ultrasonic Lamb-waves-based techniques as a basis for damage detection.

This work was done by Behzad Moslehi and Richard J. Black of Intelligent Fiber Optic Systems Corp. and Yasser Gowayed of Auburn University for Dryden Flight Research Center. Further information is contained in a TSP (see page 1). DRC-011-004

Health-Enabled Smart Sensor Fusion Technology

Stennis Space Center, Mississippi

A process was designed to fuse data from multiple sensors in order to make a more accurate estimation of the environment and overall health in an intelligent rocket test facility (IRTF), to provide reliable, high-confidence measurements for a variety of propulsion test articles.

The object of the technology is to provide sensor fusion based on a distributed

architecture. Specifically, the fusion technology is intended to succeed in providing health condition monitoring capability at the intelligent transceiver, such as RF signal strength, battery reading, computing resource monitoring, and sensor data reading. The technology also provides analytic and diagnostic intelligence at the intelligent trans-

ceiver, enhancing the IEEE 1451.x-based standard for sensor data management and distributions, as well as providing appropriate communications protocols to enable complex interactions to support timely and high-quality flow of information among the system elements.

Troubleshooting is simplified through sensor fusion that allows users to inter-

face and verify all sensors via Web-based interfaces. Confidence is improved in decisions due to the use of fusion algorithms. Performance is improved in adverse environmental conditions. Costs for setup and teardown are reduced. Re-

calibration when replacing sensors is not required as the data acquisition system can autonomously recalibrate itself. The costs for installation, maintenance, and upgrades for measurement and control systems are also reduced.

This work was done by Ray Wang of Mobitrum Corporation for Stennis Space Center. For more information, contact Ray Wang, Mobitrum Corporation, (301) 585-4040. Refer to SSC-00361.

Extended-Range Passive RFID and Sensor Tags

SAW devices and retroreflective antenna arrays are combined.

Lyndon B. Johnson Space Center, Houston, Texas

Extended-range passive radio-frequency identification (RFID) tags and related sensor tags are undergoing development. A tag of this type incorporates a retroreflective antenna array, so that it reflects significantly more signal power back toward an interrogating radio transceiver than does a comparable passive RFID tag of prior design, which does not incorporate a retroreflective antenna array. Therefore, for a given amount of power radiated by the transmitter in the interrogating transceiver, a tag of this type can be interrogated at a distance greater than that of the comparable passive RFID or sensor tag of prior design.

The retroreflective antenna array is, more specifically, a Van Atta array, named after its inventor and first published in a patent issued in 1959. In its simplest form, a Van Atta array comprises two antenna elements connected by a transmission line so that the signal received by each antenna element is reradiated by the other antenna element (see Figure 1). The phase relationships among the received and reradiated signals are such as to produce constructive interference of the reradiated signals; that is, to concentrate the reradiated signal power in a direction back toward the source. Hence, an RFID tag equipped with a Van Atta antenna array automatically tracks the interrogating transceiver. The effective gain of a Van Atta array is the same as that of a traditional phased antenna array having the same number of antenna elements. Additional pairs of antenna elements connected by equal-length transmission lines can be incorporated into a Van Atta array to increase its directionality.

Like some RFID tags heretofore commercially available, an RFID or sensor tag of the present developmental type includes one-port surface-acoustic-wave (SAW) devices. In simplified terms, the mode of operation of a basic one-port

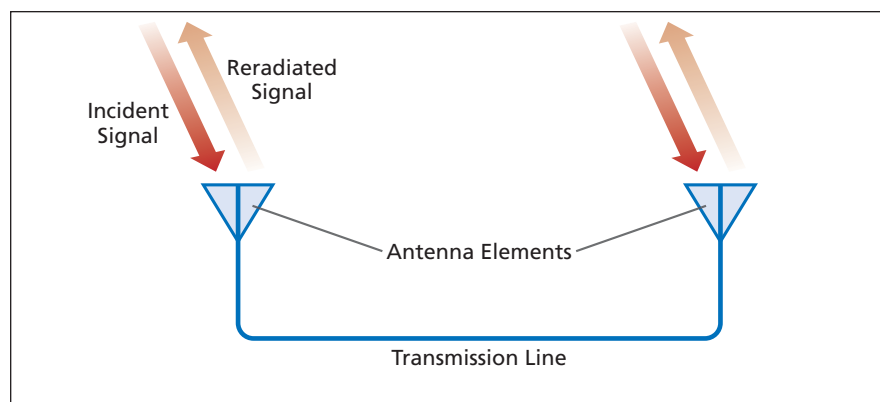


Figure 1. A Van Atta Array in its simplest form, comprising two antenna elements connected via a transmission line, exhibits partial retroreflection of an incident radio signal. If more pairs of antennas connected by equal-length transmission lines are added, the array becomes more nearly completely retroreflective.

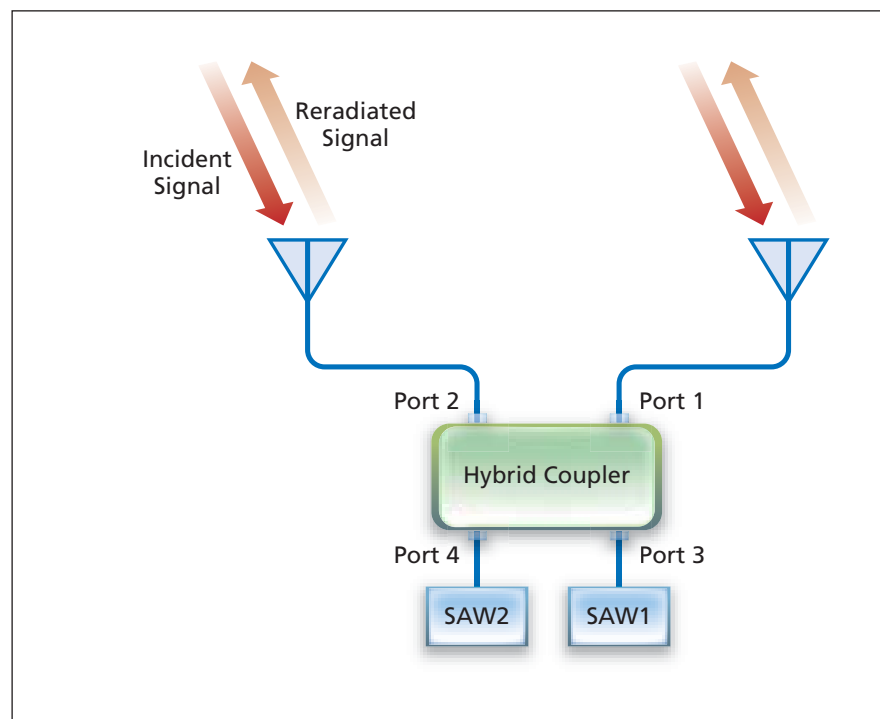


Figure 2. An Extended-Range Passive RFID or Sensor Tag in its simplest form includes two antenna elements and two SAW devices incorporated into a Van Atta array by use of a hybrid 90° coupler. A more highly directional (and, hence, longer-range) tag would incorporate additional subunits, each incorporating a similar pair of SAW devices and a similar pair of antenna elements connected via a hybrid 90° coupler.

SAW device as used heretofore in an RFID device is the following: An interrogating radio signal is converted, at an input end, from an electrical signal to an acoustic wave that propagates along a surface and encounters multiple reflectors suitably positioned along the surface. Upon returning to the input end, the reflected acoustic wave is re-converted to an electrical signal, which, in turn, is reradiated from an antenna. The distances between the reflectors in the SAW device and the corresponding times between reflections encode the identifying or sensory information onto the reradiated signal.

The fundamental problem in the present development is how to combine a Van Atta antenna array (which is inherently a multiple-port device) and one or more one-port SAW device(s) into a single, compact, passive unit that can function as a retroreflective RFID tag. The solution is to use one or more hybrid,

half-power 90° couplers. A basic unit of this type, shown in Figure 2, includes a half-power 90° hybrid coupler; two identical SAW devices (SAW1 and SAW2) connected to ports 3 and 4 of the coupler, respectively; and antenna elements connected to ports 1 and 2 of the coupler. Necessarily omitting details for the sake of brevity, it must suffice to report that the phase relationships among the coupler inputs and outputs are such as to couple the incident signal from the antenna elements to the SAW devices and couple the reflected signals from the SAW devices back to the antenna elements in the phase relationships required for a Van Atta array. Hence, the reradiated signal is automatically directed back toward the interrogating transceiver and contains identifying and/or sensory information encoded in time intervals between reflections.

An initial test of a prototype extended-range passive RFID tag of this

type containing two antennas yielded data indicative of a 37-percent increase in range over a comparable single-antenna tag. Assuming that the signal power needed to effect interrogation of a passive RFID device is proportional to the mathematical fourth power of distance, the corresponding increase in signal power needed to interrogate the single-antenna tag at the increased distance would be about 250 percent.

This work was done by Patrick W. Fink, Timothy F. Kennedy, and Gregory Y. Lin of Johnson Space Center; and Richard Barton of ERC. Further information is contained in a TSP (see page 1).

This invention is owned by NASA, and a patent application has been filed. Inquiries concerning nonexclusive or exclusive license for its commercial development should be addressed to the Patent Counsel, Johnson Space Center, (281) 483-1003. Refer to MSC-24346-1.

Hybrid Collaborative Learning for Classification and Clustering in Sensor Networks

NASA's Jet Propulsion Laboratory, Pasadena, California

Traditionally, nodes in a sensor network simply collect data and then pass it on to a centralized node that archives, distributes, and possibly analyzes the data. However, analysis at the individual nodes could enable faster detection of anomalies or other interesting events as well as faster responses, such as sending out alerts or increasing the data collection rate. There is an additional opportunity for increased performance if learners at individual nodes can communicate with their neighbors. In previous work, methods were developed by which classification algorithms deployed at sensor nodes can communicate information about event labels to each other, building on prior work with co-training, self-training, and active learning. The idea of “collaborative” learning was extended to function for clustering algorithms as well, similar to ideas from penta-training and consensus clustering. However, collaboration

between these learner types had not been explored.

A new protocol was developed by which classifiers and clusterers can share key information about their observations and conclusions as they learn. This is an active collaboration in which learners of either type can query their neighbors for information that they then use to re-train or re-learn the concept they are studying. The protocol also supports broadcasts from the classifiers and clusterers to the rest of the network to announce new discoveries.

Classifiers observe an event and assign it a label (type). Clusterers instead group observations into clusters without assigning them a label, and they collaborate in terms of pairwise constraints between two events [same-cluster (must-link) or different-cluster (cannot-link)]. Fundamentally, these two learner types speak different languages. To bridge this gap, the new communication protocol

provides four types of exchanges: hybrid queries for information, hybrid “broadcasts” of learned information, each specified for classifiers-to-clusterers, and clusterers-to-classifiers.

The new capability has the potential to greatly expand the *in situ* analysis abilities of sensor networks. Classifiers seeking to categorize incoming data into different types of events can operate in tandem with clusterers that are sensitive to the occurrence of new kinds of events not known to the classifiers. In contrast to current approaches that treat these operations as independent components, a hybrid collaborative learning system can enable them to learn from each other.

This work was done by Kiri L. Wagstaff of Caltech, Scott Sosnowski of Case Western Reserve University, and Terran Lane of the University of New Mexico for NASA's Jet Propulsion Laboratory. For more information, contact iaoffice@jpl.nasa.gov. NPO-47821



Self-Healing, Inflatable, Rigidizable Shelter

Military applications include self-sealing fuel tanks on vehicles or aircraft. Commercial applications include leak protection systems for railroad tank cars or tanker trucks carrying hazardous materials.

Marshall Space Flight Center, Alabama

Any manned missions to extraterrestrial locations will require shelter structures for a variety of purposes ranging from habitat to biomass production. Such shelters need to be constructed in such a way as to minimize stowed volume and payload weight. The structures must also be very durable and have the ability to survive punctures without collapsing. Ways of increasing available crew-load volume without greatly increasing launch weight or volume are also sought. Inflatable structures are ideal candidates for habitat structures for several reasons: (1) they feature the low stowage volume and payload weight; (2) deployed volume can be easily increased without large increases in launch weight or volume; and (3) they offer unique opportunities for incorporating intelligent and/or multi-functional systems such as self-healing capability, power generation and storage, sensor systems, and radiation protection.

An inflatable, rigidizable shelter system was developed based on Rigidization on Command (ROC) technology incorporating not only the required low-stowage volume and lightweight character achieved from an inflatable/rigidizable system, but also a self-healing foam system incorporated between the rigidizable layers of the final structure to minimize the damage caused by any punctures to the structure.

The technology builds functionality into a conventional inflatable habitat structure by incorporating a light, rigidizable composite material that can be used to make up the outer shell of the habitat structure. This composite material is used to form the two outer layers of a “sandwich” structure in which the inner layer is comprised of a foam-generating system with two components designed and placed such that they will mix upon impact and quickly seal any breaches to the habitat structure, thereby preserving the internal atmosphere of the habitat. The light, rigidizable composite is comprised of a woven glass fabric impregnated with a resin specially formulated to cure upon exposure to ultraviolet (UV) light. These composites cure extremely quickly upon exposure to UV light, either from sunlight or from other UV sources including lamps and LEDs (light emitting diodes). These composites can be extremely strong and tough, depending upon which components are employed in the resin formulation.

The inner foam self-healing system is comprised of separately encapsulated layers of the two major components of urethane foams — polyol and isocyanate — containing all the necessary catalysts, surfactants, and blowing agents required for

function. The two layers are assembled next to each other and, in the event of a puncture, both layers rupture, initiating contact of the two components. The subsequent foaming is rapid and serves to rapidly seal the system. A subscale prototype demonstrator has been designed that will allow for demonstration of all aspects of this technology including deployment, UV rigidization of composite structures using LED illumination, and scaling of punctures using an encapsulated polyurethane foam system.

The encapsulated polyurethane foam system forms the functional heart of this innovation and will greatly enhance the lifetime of inflatable habitat structures on the lunar surface or elsewhere in the solar system. Encapsulating the components ensures a proper ratio of materials to achieve the foam reaction needed for sealing, and the components are chosen such that they will react quickly and with the generation of a large volume of foam in order to seal a puncture.

This work was done by Andrea Haight and Jan-Michael Gosau of Adherent Technologies, Inc., and Anshu Dixit and Dan Gleeson of ILC Dover for Marshall Space Flight Center. For more information, contact Sammy Nabors, MSFC Commercialization Assistance Lead, at sammy.a.nabors@nasa.gov. Refer to MFS-32845-1.

Improvements in Cold-Plate Fabrication

Improvements in fabrication, cooling fluid, structural parts, and components reduce weight, fabrication steps, and costs.

Lyndon B. Johnson Space Center, Houston, Texas

Five improvements are reported in cold-plate fabrication. This cold plate is part of a thermal control system designed to serve on space missions.

The first improvement is the merging of the end sheets of the cold plate with the face sheets of the structural honeycomb panel. The cold plate, which can be

a brazed assembly, uses the honeycomb face sheet as its end sheet. Thus, when the honeycomb panel is fabricated, the face sheet that is used is already part of the cold plate. In addition to reducing weight, costs, and steps, the main benefit of this invention is that it creates a more structurally sound assembly.

The second improvement involves incorporation of the header into the closure bar to pass the fluid to a lower layer. Conventional designs have used a separate header, which increases the geometry of the system. The improvement reduces the geometry, thus allowing the cold plate to fit into smaller area.

The third improvement eliminates the need of hose, tube, or manifold to supply the cooling fluid externally. The external arrangement can be easily damaged and is vulnerable to leakage. The new arrangement incorporates an internal fluid transfer tube. This allows the fluid to pass from one cold plate to the other without any exposed external features.

The fourth improvement eliminates separate fabrication of cold plate(s) and structural members followed by a process of attaching them to each other. Here, the structural member is made of material that can be brazed just as that of the cold plate. Now the

structural member and the cold plate can be brazed at the same time, creating a monolithic unit, and thus a more structurally sound assembly.

Finally, the fifth improvement is the elimination of an additional welding step that can damage the braze joints. A tube section, which is usually welded on after the braze process, is replaced with a more structurally sound configuration that can be brazed at the same time as the rest of the cold plate.

This work was done by Mark A. Zaffetti, Edmund P. Taddey, Michael B. Laurin, and Natalia Chabebe of Hamilton Sundstrand for Johnson Space Center. For further informa-

tion, contact the JSC Innovation Partnerships Office at (281) 483-3809.

Title to this invention has been waived under the provisions of the National Aeronautics and Space Act {42 U.S.C. 2457(f)} to Hamilton Sundstrand. Inquiries concerning licenses for its commercial development should be addressed to:

Hamilton Sundstrand

Space Systems International, Inc.

One Hamilton Road

Windsor Locks, CN 06096-1010

Phone No.: (860) 654-6000

Refer to MSC-24651-1/2-1/3-1/4-1/5-1, volume and number of this NASA Tech Briefs issue, and the page number.



Technique for Radiometer and Antenna Array Calibration — TRAAC

This technique provides a unique and accurate method to calibrate an antenna and radiometer system.

Marshall Space Flight Center, Alabama

Highly sensitive receivers are used to detect minute amounts of emitted electromagnetic energy. Calibration of these receivers is vital to the accuracy of the measurements. Traditional calibration techniques depend on calibration reference internal to the receivers as reference for the calibration of the observed electromagnetic energy. Such methods can only calibrate errors in measurement introduced by the receiver only. The disadvantage of these existing methods is that they cannot account for errors introduced by devices, such as antennas, used for capturing electromagnetic radiation. This severely limits the types of antennas that can be used to make measurements with a high degree of accuracy. Complex antenna systems, such as electronically steerable antennas (also known as phased arrays), while offering potentially significant advantages, suffer from a lack of a reliable and accurate calibration technique.

The present innovation provides a method to perform an end-to-end calibration of a radio frequency (RF) receiver system comprised of an antenna and a receiver. Traditional calibration techniques cannot eliminate errors in

measurement introduced by variations in antenna characteristics. The proposed invention provides a method to quantify the instantaneous, as well as long-term, variations in antenna characteristics. This technique will enable improved accuracy in measurements made using passive receiver systems and phased array systems in particular, by monitoring the performance of the antenna array by measuring the gain of the antenna electronics in real time.

The proximity of antenna elements in an array results in interaction between the electromagnetic fields radiated (or received) by the individual elements. This phenomenon is called mutual coupling. The new calibration method uses a known noise source as a calibration load to determine the instantaneous characteristics of the antenna. The noise source is emitted from one element of the antenna array and received by all the other elements due to mutual coupling. This received noise is used as a calibration standard to monitor the stability of the antenna electronics.

The proposed calibration technique makes use of five measurements. These are observations of an internal warm load, cold load (both internal to the ra-

diometer/receiver), the scene of interest, the scene of interest with the noise source emitted from the center element of the antenna array, and a known noise source injected directly into each element of the antenna array. The noise source, coupled from the central element in the array to all other elements in a square array will be symmetric. With the noise source being emitted from the central element, the mutually coupled signal will be received on the other antenna elements, combined, and used as a calibration signal to monitor any change in the RF components (low-noise amplifiers, phase shifters, attenuators, and power combiners) in front of the radiometer. Based on these observations, a calibrated estimate of the scene can be obtained.

This work was done by Paul Meyer, William Sims, Kosta Varnavas, and Jeff McCracken of Marshall Space Flight Center; Karthik Srinivasan, Ashutosh Limaye, and Charles Laymon of Universities Space Research Association; and James Richeson of ICRC. For further information, contact Sammy Nabors, MSFC Commercialization Assistance Lead, at sammy.a.nabors@nasa.gov. Refer to MFS-32783-1.

Real-Time Cognitive Computing Architecture for Data Fusion in a Dynamic Environment

This architecture can enable smart instrumentation for automotive, security, and intelligent robotics applications.

NASA's Jet Propulsion Laboratory, Pasadena, California

A novel cognitive computing architecture is conceptualized for processing multiple channels of multi-modal sensory data streams simultaneously, and fusing the information in real time to generate intelligent reaction sequences. This unique architecture is ca-

pable of assimilating parallel data streams that could be analog, digital, synchronous/asynchronous, and could be programmed to act as a knowledge synthesizer and/or an "intelligent perception" processor. In this architecture, the bio-inspired models of visual path-

way and olfactory receptor processing are combined as processing components, to achieve the composite function of "searching for a source of food while avoiding the predator." The architecture is particularly suited for scene analysis from visual data and odorant

signature identification in a heterogeneous environment.

In this architecture, there are four basic blocks: input, output, processing, and storage. The input block consists of sensing devices including IR, lidar, radar, visual, chemical, and biosensors, at their various sampling data rates. Based on application scenario, selected sensory streams are sent by the input block to the subsequent “processing” block in a fully parallel fashion. Feature data is extracted from the analog/digital sensory streams and is accumulated in the storage block for enriching the “knowledge base” as a situation unfolds. The incoming raw data is not stored as is the usual approach in current computer architecture, and is reconstructed if required during the process in real time. The output block sends the output signal to various interfaces (actuating interfaces), such as other machines, humans,

or RF devices. The processing block consists of several mathematical constructs including Principal Component Analysis (PCA), Independent Component Analysis (ICA), Neural Network (NN), Genetic Algorithm (GA), etc., and is controlled by a hierarchy of logical rules to enact reasoning, reconfiguring, and adapting as required when the target is changing in the dynamic environment. Therefore, the processing block can select an architecture for each particular application as needed, dynamically, and still remain compatible with a digital environment. The conceptualized architecture, capable of extracting knowledge from information and using the knowledge for reasoning, adapting, and reacting therefore qualifies as a cognitive architecture for real-time data fusion in a dynamic environment. Furthermore, its dynamic autonomous reconfigurability makes it versatile as a “gen-

eral-purpose” intelligent system to accomplish the “searching for a source of food while avoiding the predator” function.

This work was done by Tuan A. Duong and Vu A. Duong of Caltech for NASA’s Jet Propulsion Laboratory. Further information is contained in a TSP (see page 1).

In accordance with Public Law 96-517, the contractor has elected to retain title to this invention. Inquiries concerning rights for its commercial use should be addressed to:

*Innovative Technology Assets Management
JPL*

Mail Stop 202-233

4800 Oak Grove Drive

Pasadena, CA 91109-8099

E-mail: iaoffice@jpl.nasa.gov

Refer to NPO-46633, volume and number of this NASA Tech Briefs issue, and the page number.

Programmable Digital Controller

Goddard Space Flight Center, Greenbelt, Maryland

An existing three-channel analog servo loop controller has been redesigned for piezoelectric-transducer-based (PZT-based) etalon control applications to a digital servo loop controller. This change offers several improvements over the previous analog controller, including software control over proportional–integral–derivative (PID) parameters, inclusion of other data of interest such as temperature and pressure in the control laws, improved ability to compensate for PZT hysteresis and mechanical mount fluctuations, ability to provide pre-programmed scanning and stepping routines, improved user interface, expanded data acquisition, and reduced size, weight, and power.

The original analog servo controller only had the ability to correct for a sin-

gle error term generated by the capacitive gap sensor. This was less than optimal when trying to return to the same gap position due to the hysteresis of the PZT motors and thermal drift in the electronics.

To overcome the limitations of the analog servo loop, it was decided that a control loop could be built around a microcontroller/central processing unit (CPU), i.e., a digital servo loop. The CPU would query various sensors such as a capacitive gap sensor or temperature sensor, among others, then based on re-programmable control laws, provide a driving signal to a high-voltage driver that actuates the PZT motor on the etalon. The system is based on mostly COTS (commercial off-the-shelf) hardware and software.

The design is based around a new generation of direct capacitance to digital converters from Analog Devices, the AD7745. This integrated circuit (IC) allows the measurement of the capacitance of the gap capacitor at up to 90 Hz with resolutions down to 4 aF. This measurement is an absolute value whereas the previous analog design measured capacitance relative to a reference capacitor whose value had some uncertainty. The new design allows one to measure the gap directly, after calibration, thereby greatly improving overall control.

This work was done by Gregory J. Wassick of Michigan Aerospace Corporation for Goddard Space Flight Center. For further information, contact the Goddard Innovative Partnerships Office at (301) 286-5810. GSC-15524-1

Use of CCSDS Packets Over SpaceWire to Control Hardware

Goddard Space Flight Center, Greenbelt, Maryland

For the Lunar Reconnaissance Orbiter, the Command and Data Handling subsystem consisted of several electronic hardware assemblies that were connected with SpaceWire serial links. Electronic hardware would be commanded/controlled and telemetry data was obtained using the SpaceWire links. Prior art focused on par-

allel data buses and other types of serial buses, which were not compatible with the SpaceWire and the core flight executive (CFE) software bus.

This innovation applies to anything that utilizes both SpaceWire networks and the CFE software. The CCSDS (Consultative Committee for Space Data Systems)

packet contains predetermined values in its payload fields that electronic hardware attached at the terminus of the SpaceWire node would decode, interpret, and execute. The hardware’s interpretation of the packet data would enable the hardware to change its state/configuration (command) or generate status (telemetry).

The primary purpose is to provide an interface that is compatible with the hardware and the CFE software bus. By specifying the format of the CCSDS packet, it is possible to specify how the resulting hardware is to be built (in terms of digital logic) that results in a hardware design that can be controlled by the CFE software bus in the final application.

The component parts are the CFE, the electronic hardware attached at the terminus of the SpaceWire link, and the SpaceWire link itself. The CCSDS packet is what is produced by the CFE for control of the hardware as well as obtaining status.

The main benefits of this innovation are the ability to re-use existing CFE flight software code, the hardware responds to

“native” CCSDS packets instead of going through a translation layer, and it provides a mechanism to control hardware features using software constructs.

This work was done by Omar Haddad, Michael Blau, Noosha Haghani, William Yuknis, and Dennis Albaijes of Goddard Space Flight Center. Further information is contained in a TSP (see page 1). GSC-15981-1



Key Decision Record Creation and Approval Module

Retaining good key decision records is critical to ensuring the success of a project or operation. Having adequately documented decisions with supporting documents and rationale can greatly reduce the amount of rework or reinvention over a project's, vehicle's, or facility's lifecycle. Stennis Space Center developed and uses a software tool that automates the Key Decision Record (KDR) process for its engineering and test projects. It provides the ability for a user to log key decisions that are made during the course of a project. By customizing Parametric Technology Corporation's (PTC) Windchill product, the team was able to log all information about a decision, and electronically route that information for approval. Customizing the Windchill product allowed the team to directly connect these decisions to the engineering data that it might affect and notify data owners of the decision. The user interface was created in JSP and Javascript, within the OOTB (Out of the Box) Windchill product, allowing users to create KDRs. Not only does this interface allow users to create and track KDRs, but it also plugs directly into the OOTB ability to associate these decision records with other relevant engineering data such as drawings, designs, models, requirements, or specifications.

This work was done by Bartt Hebert and Elizabeth A. Messer of Stennis Space Center; Colby Albasini of Computer Sciences Corp.; and Thang Le, William O'Rourke, Sr., Tim Stiglets, and Ted Strain of Sai Tech Inc. Inquiries concerning rights for the commercial use of this invention should be addressed to the Intellectual Property Manager at Stennis Space Center (228) 688-1929. SSC-00338

Enhanced Graphics for Extended Scale Range

Enhanced Graphics for Extended Scale Range is a computer program for rendering fly-through views of scene models that include visible objects differing in size by large orders of magnitude. An example would be a scene showing a person in a park at night with the moon, stars, and galaxies in the background sky. Prior graphical computer programs exhibit

arithmetic and other anomalies when rendering scenes containing objects that differ enormously in scale and distance from the viewer.

The present program dynamically repartitions distance scales of objects in a scene during rendering to eliminate almost all such anomalies in a way compatible with implementation in other software and in hardware accelerators. By assigning depth ranges corresponding to rendering precision requirements, either automatically or under program control, this program spaces out object scales to match the precision requirements of the rendering arithmetic. This action includes an intelligent partition of the depth buffer ranges to avoid known anomalies from this source. The program is written in C++, using OpenGL, GLUT, and GLUI standard libraries, and nVidia GeForce Vertex Shader extensions. The program has been shown to work on several computers running UNIX and Windows operating systems.

This program was written by Andrew J. Hanson and Philip Chi-Wing Fu of Indiana University for Goddard Space Flight Center. Further information is contained in a TSP (see page 1). GSC-14819-1

Debris Examination Using Ballistic and Radar Integrated Software

The Debris Examination Using Ballistic and Radar Integrated Software (DEBRIS) program was developed to provide rapid and accurate analysis of debris observed by the NASA Debris Radar (NDR). This software provides a greatly improved analysis capacity over earlier manual processes, allowing for up to four times as much data to be analyzed by one-quarter of the personnel required by earlier methods. There are two applications that comprise the DEBRIS system: the Automated Radar Debris Examination Tool (ARDENT) and the primary DEBRIS tool.

The debris radars were established to provide insight into debris events for all future space shuttle flights. Often, the debris particles are either too small or moving too quickly to be accurately characterized in any other way. Data must be rapidly and accurately analyzed in order

to assess the threat environment from ascent debris. The DEBRIS tools offer that capability, and were specifically tailored to the needs of the debris analysis mission.

The ARDENT application is intended to autonomously identify, characterize, annotate, and perform statistics on debris tracks from 150 seconds after launch to loss of signal at the far horizon. The DEBRIS application is intended primarily for analysis of the data within the first 150 seconds of flight. It allows the user to explore the available data and annotate observed debris events and tracks. It also allows ballistic analysis of an annotated event, and allows the user to display all annotated events for the mission and the associated meta information for those events.

The ARDENT debris detection algorithm uses a Multi-scale Localized Radon Transform (MSLRT) optimized for this application. The MSLRT computes a localized Radon transform of blocks of the data for multiple block sizes (or scales) to form an aggregated (across scales) debris track detection map based on identifying piece-wise linear features in the data. The DEBRIS tool consolidates and extends the capability of several discrete applications developed early in the NDR technology maturation process; specifically, data viewing, annotation of candidate debris events, and various elements of trajectory analysis. This consolidation dramatically streamlines the analysis process and the amount of overhead in both time and effort needed to fully process the debris risk portion of the shuttle ascent.

The ballistic and radar signature products of these tools allow assessment of debris material type, shape, size, and release location — information that is used to determine threat to the current mission as well as flight safety for future missions. The analysis efficiencies afforded by these tools allow detailed threat assessment of tens of gigabytes of data within three days of launch.

This work was done by Anthony Griffith, Matthew Schottel, David Lee, Robert Scully, and Joseph Hamilton of Johnson Space Center; Brian Kent, Christopher Thomas, Jonathan Benson, and Eric Branch of the U.S. Air Force; and Paul Hardman and Martin Stuble of NAVAIR (Patuxent) Department of the Navy. MSC-24827-1

2 Data Distribution System (DDS) and Solar Dynamic Observatory Ground Station (SDOGS) Integration Manager

The DDS SDOGS Integration Manager (DSIM) provides translation between native control and status formats for systems within DDS and SDOGS, and the ASIST (Advanced Spacecraft Integration and System Test) control environment in the SDO MOC (Solar Dynamics Observatory Mission Operations Center).

This system was created in response for a need to centralize remote monitor and control of SDO Ground Station equipments using ASIST control environment in SDO MOC, and to have configurable table definition for equipment. It provides translation of status and monitoring information from the native systems into ASIST-readable format to display on pages in the MOC.

The manager is lightweight, user friendly, and efficient. It allows data trending, correlation, and storing. It allows using ASIST as common interface for remote monitor and control of heterogeneous equipments. It also provides fail-over capability to back up machines.

This work was done by Kim Pham and Thomas Bialas of Goddard Space Flight Center. Further information is contained in a TSP (see page 1). GSC-16020-1

2 Eclipse-Free-Time Assessment Tool for IRIS

IRIS_EFT is a scientific simulation that can be used to perform an Eclipse-Free-Time (EFT) assessment of IRIS (Infrared Imaging Surveyor) mission orbits. EFT is defined to be those time intervals longer than one day during which the IRIS spacecraft is not in the Earth's shadow. Program IRIS_EFT implements a special perturbation of orbital motion to numerically integrate Cowell's form of the system of differential equations. Shadow conditions are predicted by embedding this integrator within Brent's method for finding the root of a nonlinear equation. The IRIS_EFT software models the effects of the following types of orbit perturbations on the long-term evolution and shadow characteristics of IRIS mission orbits:

- Non-spherical Earth gravity,
- Atmospheric drag,
- Point-mass gravity of the Sun, and
- Point-mass gravity of the Moon.

The objective of this effort was to create an in-house computer program that would perform eclipse-free-time analysis

of candidate IRIS spacecraft mission orbits in an accurate and timely fashion. The software is a suite of Fortran subroutines and data files organized as a "computational" engine that is used to accurately predict the long-term orbit evolution of IRIS mission orbits while searching for Earth shadow conditions.

The core algorithms of this software product have been used to solve a variety of unique orbital mechanics and targeting problems. Past applications include lunar shadow requirements for Chandra, perigee decay of geosynchronous transfer orbits due to third-body point-mass perturbations, and prediction of orbital lifetime and decay of Earth satellites.

This work was done by David Eagle of a.i. solutions Inc. for Kennedy Space Center. For additional information, contact David Eagle at (321) 867-8913. KSC-13519

2 Automated and Manual Rocket Crater Measurement Software

An update has been performed to software designed to do very rapid automated measurements of craters created in sandy substrates by rocket exhaust on liftoff. The previous software was optimized for pristine lab geometry and lighting conditions. This software has been enhanced to include a section for manual measurements of crater parameters; namely, crater depth, crater full width at half max, and estimated crater volume. The tools provide a very rapid method to measure these manual parameters to ease the burden of analyzing large data sets.

This software allows for rapid quantization of the rocket crater parameters where automated methods may not work. The progress of spreadsheet data is continuously saved so that data is never lost, and data can be copied to clipboards and pasted to other software for analysis. The volume estimation of a crater is based on the central max depth axis line, and the polygonal shape of the crater is integrated around that axis.

This work was done by Philip Metzger of Kennedy Space Center and Christopher Immer of ASRC Aerospace Corp. Further information is contained in a TSP (see page 1). KSC-13386

2 MATLAB Stability and Control Toolbox Trim and Static Stability Module

MATLAB Stability and Control Toolbox (MASCOT) utilizes geometric, aerodynamic, and inertial inputs to cal-

culate air vehicle stability in a variety of critical flight conditions. The code is based on fundamental, non-linear equations of motion and is able to translate results into a qualitative, graphical scale useful to the non-expert.

MASCOT was created to provide the conceptual aircraft designer accurate predictions of air vehicle stability and control characteristics. The code takes as input mass property data in the form of an inertia tensor, aerodynamic loading data, and propulsion (i.e. thrust) loading data. Using fundamental non-linear equations of motion, MASCOT then calculates vehicle trim and static stability data for the desired flight condition(s). Available flight conditions include six horizontal and six landing rotation conditions with varying options for engine out, crosswind, and sideslip, plus three take-off rotation conditions. Results are displayed through a unique graphical interface developed to provide the non-stability and control expert conceptual design engineer a qualitative scale indicating whether the vehicle has acceptable, marginal, or unacceptable static stability characteristics. If desired, the user can also examine the detailed, quantitative results.

This work was done by Sean P. Kenny of Langley Research Center and Luis Crespo of the National Institute of Aerospace. Further information is contained in a TSP (see page 1). LAR-17483-1

2 Patched Conic Trajectory Code

PatCon code was developed to help mission designers run trade studies on launch and arrival times for any given planet. Initially developed in Fortran, the required inputs included launch date, arrival date, and other orbital parameters of the launch planet and arrival planets at the given dates. These parameters include the position of the planets, the eccentricity, semi-major axes, argument of periapsis, ascending node, and inclination of the planets. With these inputs, a patched conic approximation is used to determine the trajectory.

The patched conic approximation divides the planetary mission into three parts: (1) the departure phase, in which the two relevant bodies are Earth and the spacecraft, and where the trajectory is a departure hyperbola with Earth at the focus; (2) the cruise phase, in which the two bodies are the Sun and the spacecraft, and where the trajectory is a transfer el-

lipse with the Sun at the focus; and (3) the arrival phase, in which the two bodies are the target planet and the spacecraft, where the trajectory is an arrival hyperbola with the planet as the focus.

This work was done by Brooke Anderson Park and Henry Wright of Langley Research Center. Further information is contained in a TSP (see page 1). LAR-17446-1

Ring Image Analyzer

Ring Image Analyzer software analyzes images to recognize elliptical patterns. It determines the ellipse parameters (axes ratio, centroid coordinate, tilt angle). The program attempts to recognize elliptical fringes (e.g., Newton Rings) on a photograph and determine their centroid position, the short-to-long-axis ratio, and the angle of rotation of the long axis relative to the horizontal direction on the photograph. These capabilities are important in interferometric imaging and control of surfaces. In particular, this program has been developed and applied for determining the rim shape of precision-machined optical whispering gallery mode resonators.

The program relies on a unique image recognition algorithm aimed at recognizing elliptical shapes, but can be easily adapted to other geometric shapes. It is

robust against non-elliptical details of the image and against noise.

Interferometric analysis of precision-machined surfaces remains an important technological instrument in hardware development and quality analysis. This software automates and increases the accuracy of this technique. The software has been developed for the needs of an R&TD-funded project and has become an important asset for the future research proposal to NASA as well as other agencies.

This work was done by Dmitry V. Strelakov of Caltech for NASA's Jet Propulsion Laboratory. Further information is contained in a TSP (see page 1). This software is available for commercial licensing. Please contact Daniel Broderick of the California Institute of Technology at danielb@caltech.edu. Refer to NPO-47579.

SureTrak Probability of Impact Display

The SureTrak Probability of Impact Display software was developed for use during rocket launch operations. The software displays probability of impact information for each ship near the hazardous area during the time immediately preceding the launch of an unguided vehicle.

Wallops range safety officers need to be sure that the risk to humans is below a cer-

tain threshold during each use of the Wallops Flight Facility Launch Range. Under the variable conditions that can exist at launch time, the decision to launch must be made in a timely manner to ensure a successful mission while not exceeding those risk criteria. Range safety officers need a tool that can give them the needed probability of impact information quickly, and in a format that is clearly understandable. This application is meant to fill that need.

The software is a reuse of part of software developed for an earlier project: Ship Surveillance Software System (S4). The S4 project was written in C++ using Microsoft Visual Studio 6. The data structures and dialog templates from it were copied into a new application that calls the implementation of the algorithms from S4 and displays the results as needed. In the S4 software, the list of ships in the area was received from one local radar interface and from operators who entered the ship information manually. The SureTrak Probability of Impact Display application receives ship data from two local radars as well as the SureTrak system, eliminating the need for manual data entry.

This work was done by John Elliott of Goddard Space Flight Center. Further information is contained in a TSP (see page 1). GSC-16064-1



Implementation of a Non-Metallic Barrier in an Electric Motor

Lyndon B. Johnson Space Center, Houston, Texas

Electric motors that run in pure oxygen must be sealed, or “canned,” for safety reasons to prevent the oxygen from entering into the electrical portion of the motor. The current canning process involves designing a metallic barrier around the rotor to provide the separation. This metallic barrier reduces the motor efficiency as speed is increased. In higher-speed electric motors, efficiency is greatly improved if a very thin, non-metallic barrier can be utilized. The barrier thickness needs to be approximately 0.025-in. ($\approx 0.6\text{-mm}$) thick and can be made of a brittle material such as glass. The motors, however, designed for space applications are typically subject to high-vibration environments.

A fragile, non-metallic barrier can be utilized in a motor assembly if held in place by a set of standard rubber O-ring seals. The O-rings provide the necessary sealing to keep oxygen away from the electrical portion of the motor and also isolate the fragile barrier from the harsh motor vibration environment. The compliance of the rubber O-rings gently constrains the fragile barrier and isolates it from the harsh external motor environment. The use of a non-metallic barrier greatly improves motor performance, especially at higher speeds, while isolating the electronics from the working fluid with an inert liner.

This work was done by George M'Sadoques, Michael Carra, and Woody Beringer of

Hamilton Sundstrand for Johnson Space Center. For further information, contact the JSC Innovation Partnerships Office at (281) 483-3809.

Title to this invention has been waived under the provisions of the National Aeronautics and Space Act (42 U.S.C. 2457(f)) to Hamilton Sundstrand. Inquiries concerning licenses for its commercial development should be addressed to:

*Hamilton Sundstrand
Space Systems International, Inc.
One Hamilton Road
Windsor Locks, CT 06096-1010
Phone No.: (860) 654-6000*

Refer to MSC-24876-1, volume and number of this NASA Tech Briefs issue, and the page number.

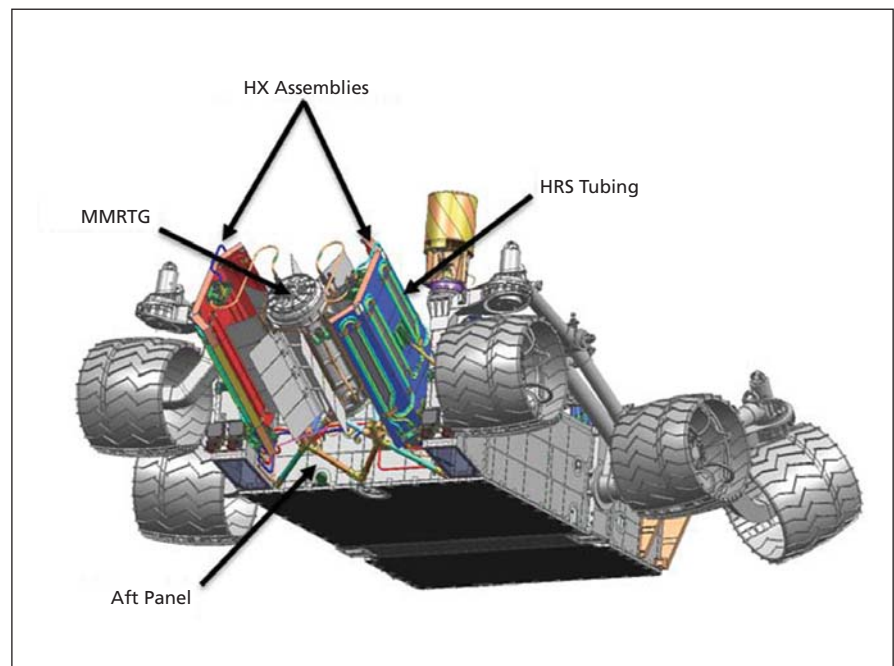
Multi-Mission Radioisotope Thermoelectric Generator Heat Exchangers for the Mars Science Laboratory Rover

These heat exchangers can be used in any application in which heat loads must be simultaneously collected and rejected from opposite sides of the same structure.

NASA's Jet Propulsion Laboratory, Pasadena, California

The addition of the Multi-Mission Radioisotope Thermoelectric Generator (MMRTG) to the Mars Science Laboratory (MSL) Rover requires an advanced thermal control system that is able to both recover and reject the waste heat from the MMRTG as needed in order to maintain the onboard electronics at benign temperatures despite the extreme and widely varying environmental conditions experienced both on the way to Mars and on the Martian surface (See figure).

Based on the previously successful Mars landed mission thermal control schemes, a mechanically pumped fluid loop (MPFL) architecture was selected as the most robust and efficient means for meeting the MSL thermal requirements. The MSL heat recovery and rejection system (HRS) is comprised of two Freon (CFC-11) MPFLs that interact closely with one another to provide comprehensive thermal management throughout all mission phases. The first loop, called the Rover HRS (RHRS), consists of a set of pumps,



MSL Rover in Stowed Cruise Configuration showing HXs positioned on both sides of finned MMRTG.

thermal control valves, and heat exchangers (HXs) that enables the transport of heat from the MMRTG to the rover electronics during cold conditions or from the electronics straight to the environment for immediate heat rejection during warm conditions. The second loop, called the Cruise HRS (CHRS), is thermally coupled to the RHRS during the cruise to Mars, and provides a means for dissipating the waste heat more directly from the MMRTG as well as from both the cruise stage and rover avionics by promoting circulation to the cruise stage radiators.

A multifunctional structure was developed that is capable of both collecting waste heat from the MMRTG and reject-

ing the waste heat to the surrounding environment. It consists of a pair of honeycomb core sandwich panels with HRS tubes bonded to both sides. Two similar HX assemblies were designed to surround the MMRTG on the aft end of the rover. Heat acquisition is accomplished on the interior (MMRTG facing) surface of each HX while heat rejection is accomplished on the exterior surface of each HX. Since these two surfaces need to be at very different temperatures in order for the fluid loops to perform efficiently, they need to be thermally isolated from one another. The HXs were therefore designed for high in-plane thermal conductivity and extremely low

through-thickness thermal conductivity by using aluminum facesheets and aerogel as insulation inside a composite honeycomb core. Complex assemblies of hand-welded and uniquely bent aluminum tubes are bonded onto each side of the HX panels, and are specifically designed to be easily mated and demated to the rest of the RHRS in order to ease the integration effort.

This work was done by A. J. Mastropietro, John S. Beatty, Frank P. Kelly, Pradeep Bhandari, David P. Bame, Yuanming Liu, Gajanana C. Birur, Jennifer R. Miller, Michael T. Pauken, and Peter M. Illsley of Caltech for NASA's Jet Propulsion Laboratory. For more information, contact iaoffice@jpl.nasa.gov. NPO-47619

❁ Uniform Dust Distributor for Testing Radiative Emittance of Dust-Coated Surfaces

This device could be used in applying uniform amounts of dust on surfaces to which coatings may be applied.

Lyndon B. Johnson Space Center, Houston, Texas

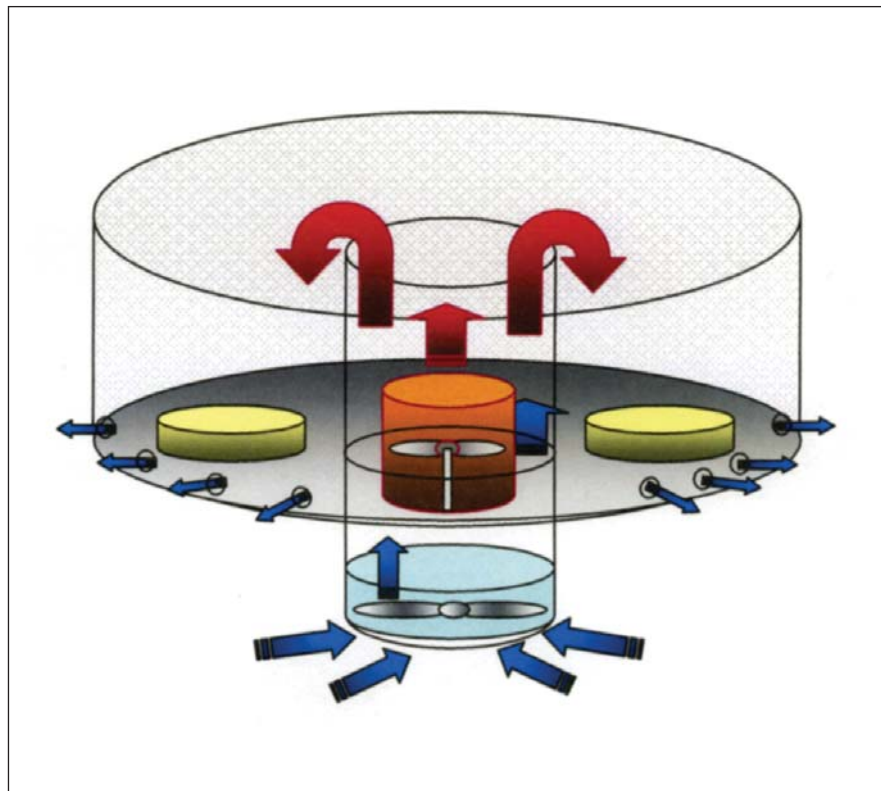
This apparatus distributes dust (typical of the Martian surface) in a uniform fashion on the surface of multiple samples simultaneously. The primary innovation is that the amount of dust deposited on the multiple surfaces can be controlled by the time that the apparatus operates, and each sample will be subject to the same amount of dust deposition. The exact weight of dust that is added per unit of sample area is determined by the use of slides that can be removed sequentially after each dusting.

The objective was to produce the same weight of dust per unit sample area on each of eight samples that were part of an apparatus that measured the effective radiative emittance of dust-coated surfaces. The uniformity of dust deposition across all the samples was to be maintained as additional layers of dust were added. The unique nature of this problem is that the dust deposition was required to be spatially uniform on each sample, and deposited equally on all samples subjected to the dusting process. The dusting device also had to be movable so that after a dust layer is applied, the device could be removed and the samples could remain stationary in the experimental apparatus. In this way, the dust layer was not disturbed throughout the course of the experiments.

The dusting device comprises three parts: an aluminum sample table on

which the samples are placed, a Plexiglas aerator tube that contains a fan and the dust aerator, and a chamber top for containment. The table supports the cham-

ber top and the aerator tube as dusting is performed. The tube and the chamber top are removed after each dust layer is applied.



Schematic depiction of the **Dusting Apparatus**. Dust is placed in central reservoir (orange container). The impeller on the bottom (blue) creates an air/dust suspension, which rises slowly (red arrows) in the tube surrounding the reservoir. The suspension settles on the coupons (yellow) below.

Test samples are arrayed uniformly around the table and the hole in the center admits the aerator tube and assures repeatable vertical alignment. A groove around the periphery of the table allows repeatable alignment of the chamber top with the table. Microscope slides are

placed between samples on the table so that once dusting has been performed, they can be removed and weighed to determine the weight of dust per unit area added to the samples. As additional dusting is done, additional slides are removed and weighed so that the amount

of dust that accumulates with multiple dustings can be determined.

This work was done by Kathryn Miller Hurlbert of Johnson Space Center, and Larry C. Witte and D. Keith Hollingsworth of the University of Houston. Further information is contained in a TSP (see page 1). MSC-23944-1

MicroProbe Small Unmanned Aerial System

Goddard Space Flight Center, Greenbelt, Maryland

The MicroProbe unmanned aerial system (UAS) concept incorporates twin electric motors mounted on the vehicle wing, thus enabling an aerodynamically and environmentally clean nose area for atmospheric sensors. A payload bay is also incorporated in the

fuselage to accommodate remote sensing instruments.

A key feature of this concept is lightweight construction combined with low flying speeds to minimize kinetic energy and associated hazards, as well as maximizing spatial resolution. This type of

aerial platform is needed for Earth science research and environmental monitoring. There were no vehicles of this type known to exist previously.

This work was done by Geoffrey Bland and Ted Miles of Goddard Space Flight Center. GSC-16206-1



Highly Stable and Active Catalyst for Sabatier Reactions

Lyndon B. Johnson Space Center, Houston, Texas

Highly active Ru/TiO₂ catalysts for Sabatier reaction have been developed. The catalysts have shown to be stable under repeated shutting down/startup conditions. When the Ru/TiO₂ catalyst is coated on the engineered substrate Fe-

CrAlY felt, activity enhancement is more than doubled when compared with an identically prepared engineered catalyst made from commercial Degussa catalyst. Also, bimetallic Ru-Rh/TiO₂ catalysts show high activity at high throughput.

This work was done by Jianli Hu and Kriston P. Brooks of Battelle Memorial Institute for Johnson Space Center. For further information, contact the JSC Innovation Partnerships Office at (281) 483-3809. MSC-24299-1

Better Proton-Conducting Polymers for Fuel-Cell Membranes

These materials could function while hotter and drier.

NASA's Jet Propulsion Laboratory, Pasadena, California

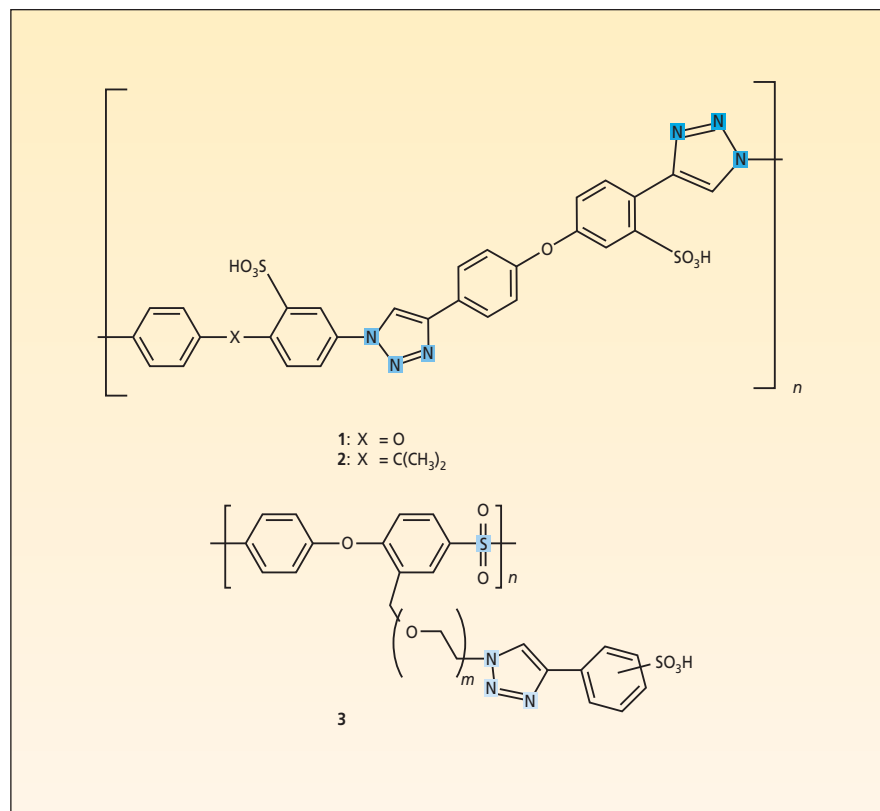
Polyoxyphenylene triazole sulfonic acid has been proposed as a basis for development of improved proton-conducting polymeric materials for solid-electrolyte membranes in hydrogen/air fuel cells. Heretofore, the proton-conducting membrane materials of choice have been exemplified by a family of perfluorosulfonic acid-based polymers (Nafion[®] or equivalent). These materials are suitable for operation in the temperature of 75 to 85 °C, but in order to reduce the sizes and/or increase the energy-conversion efficiencies of fuel-cell systems, it would be desirable to increase temperatures to as high as 120 °C for transportation applications, and to as high as 180 °C for stationary applications. However, at 120 °C and at relative humidity values below 50 percent, the loss of water from perfluorosulfonic acid-based polymer membranes results in fuel-cell power densities too low to be of practical value. Therefore, membrane electrolyte materials that have usefully high proton conductivity in the temperature range of 180 °C at low relative humidity and that do not rely on water for proton conduction at 180 °C would be desirable.

The proposed polyoxyphenylene triazole sulfonic acid-based materials have been conjectured to have these desirable properties. These materials would be free of volatile or mobile acid constituents. The generic molecular structure of these materials is intended to exploit the fact, demonstrated in previous research, that materials that contain ionizable acid and base groups covalently

attached to thermally stable polymer backbones exhibit proton conduction even in the anhydrous state.

The sulfonic acid group in polyoxyphenylene triazole sulfonic acid is a

strong acid capable of generating protons when presented with a suitable base. The triazole moiety offers at least three base sites for protonation. The polyoxyphenylene backbone is endowed



These **Three Generic Molecular Structures** are representative of the proposed polyoxyphenylene triazole sulfonic acid-based compounds. The subscripts *m* and *n* denote integers. These compounds as denoted by their full names are (1) poly[(1H-1,2,3-triazole-1,4-diyl)-co-(oxyphenylenesulfonic acid)], (2) poly[(1H-1,2,3-triazole-1,4-diyl)-co-bisphenylenesulfonic acid]-co-(oxyphenylenesulfonic acid)], and (3) poly[(oxyphenylenesulfone)-graft-1-(1H-1,2,3-triazole-1,4-diyl)-1-poly(ethylene oxide)-4-benzenesulfonic acid)].

with excellent thermal stability, as evidenced by the numerous engineering polymers, incorporating this and related backbones, that can withstand operating temperatures up to 300 °C. Also, polymers that have similar backbones [poly(arylene ether ether ketone) and poly(arylene ether sulfone)] have been reported to be electrochemically stable. Hence, the proposed polymers are expected to exhibit high thermal and electrochemical stability.

Below the boiling temperature of water, the proposed materials could absorb and retain water and could conduct protons by means of the same physical mechanisms as those of prior membrane electrolyte materials that rely on water.

Above the boiling temperature of water, membranes become dehydrated, but membranes made of the proposed materials could still conduct protons by transfer between the acid and base groups on the polymer backbones. Hence, the proposed polymers are expected to conduct protons under anhydrous as well as hydrous conditions.

The figure depicts generic molecular structures of three types of compounds according to the proposal. These compounds could be synthesized from commercially available starting compounds and/or from intermediate compounds that can be synthesized from commercially available starting compounds.

This work was done by Sri Narayan of Caltech and Prakash Reddy of the University of Missouri-Rolla for NASA's Jet Propulsion Laboratory. For more information, contact iaoffice@jpl.nasa.gov.

In accordance with Public Law 96-517, the contractor has elected to retain title to this invention. Inquiries concerning rights for its commercial use should be addressed to:

*Innovative Technology Assets Management
JPL*

Mail Stop 202-233

4800 Oak Grove Drive

Pasadena, CA 91109-8099

E-mail: iaoffice@jpl.nasa.gov

Refer to NPO-44760, volume and number of this NASA Tech Briefs issue, and the page number.



CCD Camera Lens Interface for Real-Time Theodolite Alignment

The lens simulates the human eye and creates an improved way to align a system.

Goddard Space Flight Center, Greenbelt, Maryland

Theodolites are a common instrument in the testing, alignment, and building of various systems ranging from a single optical component to an entire instrument. They provide a precise way to measure horizontal and vertical angles. They can be used to align multiple objects in a desired way at specific angles. They can also be used to reference a specific location or orientation of an object that has moved. Some systems may require a small margin of error in position of components. A theodolite can assist with accurately measuring and/or minimizing that error.

Previously, when aligning a system with a theodolite, it required the user to use their unaided eye with the theodolite eyepiece. When viewing the alignment through the eyepiece, the user could induce human error by how well they could see the alignment indicators. Other attempts have used a bare CCD (charge

coupled device) array attached to the theodolite, but this technique limited the ability to achieve proper focus of the theodolite because it did not properly simulate the human eye, and therefore introduced error.

This technology minimizes time required to align a system with a Leica WildT3000 Theodolite or multiple theodolites. The secondary objective was to allow a single individual to align a single coupled system to multiple theodolites, simultaneously, in real time. This technology mounts a CCD camera with a lens at the theodolite eyepiece. This simulates the human eye and creates an improved way to align a system with the theodolite by increasing accuracy and adding the ability to record alignment quantitatively.

The technology is an adapter for a CCD camera with lens to attach to a Leica Wild T3000 Theodolite eyepiece that enables viewing on a connected monitor, and thus

can be utilized with multiple theodolites simultaneously. This technology removes a substantial part of human error by relying on the CCD camera and monitors. It also allows image recording of the alignment, and therefore provides a quantitative means to measure such error.

This method allows a fast and accurate method of alignment and minimizes the need for multiple individuals to perform alignment of multiple theodolites. It also eliminates the need to look through the eyepiece of the theodolite, thus eliminating the chance of eye injury when dealing with high-intensity light sources. This method allows the ability to place the theodolite in constrained locations that someone using the traditional human eye technique could not do.

This work was done by Shane Wake and V. Stanley Scott, III of Goddard Space Flight Center. Further information is contained in a TSP (see page 1). GSC-16175-1

Peregrine 100-km Sounding Rocket Project

The objective is to design, build, test, and fly a stable, efficient liquefying fuel hybrid rocket.

Ames Research Center, Moffett Field, California

The Peregrine Sounding Rocket Program is a joint basic research program of NASA Ames Research Center, NASA Wallops, Stanford University, and the Space Propulsion Group, Inc. (SPG). The goal is to determine the applicability of this technology to a small launch system. The approach is to design, build, and fly a stable, efficient liquefying fuel hybrid rocket vehicle to an altitude of 100 km. The program was kicked off in October of 2006 and has seen considerable progress in the subsequent 18 months.

Within this period significant progress was made, including:

- Successfully completed Conceptual Design Review (CoDR) and Preliminary Design Review (PDR) for flight vehicle

capable of 100-km altitude;

- Designed and fabricated flight-weight combustion chamber, main oxidizer valve, throttle system, and thrust structure;
- Successfully completed CoDR, preliminary design review (PDR), Critical Design Review (CDR), and Integrated Test Readiness Review (ITRR) for ground test facility at NASA Ames Research Center;
- Completed subsystem testing for flight weight main oxidizer valve, throttle system, helium pressurization system, ignition system, and thrust structure;
- Completed facility integrated test series including five cold-flow tests, two with live igniters, and three hot-fire tests;
- Successfully fired motor ten times, in-

cluding one full duration burn during 1st phase of ground testing.

While this was a significant progress by any measure, the project suffered a schedule setback due to the July 2007 explosion at the Scaled Composites test site involving nitrous oxide. A thorough review of the system design and nitrous oxide operational procedures was undertaken and several changes have been implemented to increase human safety.

This research group began studying liquifying hybrid rocket fuel technology more than a decade ago. The overall goal of the research was to gain a better understanding of the fundamental physics of the liquid layer entrainment process responsible for the large increase

in regression rate observed in these fuels, and to demonstrate the effect of increased regression rate on hybrid rocket motor performance. At the time of this reporting, more than 400 motor tests were conducted with a variety of oxidizers (N_2O , GOx , LOx) at ever increasing scales with thrust levels from 5 to over 15,000 pounds (22 N to over 66 kN) in order to move this technology from the laboratory to practical applications.

The Peregrine program is the natural next step in this development. A number of small sounding rockets with diam-

eters of 3, 4, and 6 in. (7.6, 10.2, and 15.2 cm) have been flown, but Peregrine at a diameter of 15 in. (38.1 cm) and 14,000-lb (62.3-kN) thrust is by far the largest system ever attempted and will be one of the largest hybrids ever flown. Successful Peregrine flights will set the stage for a wide range of applications of this technology. The metrics of the program are:

- Demonstrate satisfactory motor performance in ground test.
- Demonstrate motor throttling in ground test.

- Fabricate the sounding rocket system, transport it to the NASA Wallops facility, and launch a payload to 100 km using paraffin and N_2O as the propellants.
- Demonstrate operational efficiency at the Wallops launch site.

This work was done by Gregory Zilliac of Ames Research Center. Further information is contained in a TSP (see page 1).

Inquiries concerning rights for commercial use of this invention should be addressed to the Ames Technology Partnerships Division at (650) 604-5761. Refer to ARC-16240-1.

SOFIA Closed- and Open-Door Aerodynamic Analyses

A series of important evaluations are completed.

Dryden Flight Research Center, Edwards, California

Work to evaluate the aerodynamic characteristics and the cavity acoustic environment of the SOFIA (Stratospheric Observatory for Infrared Astronomy) airplane has been completed. The airplane has been evaluated in its closed-door configuration, as well as several open-door configurations (see figure). Work performed included: acoustic analysis tool development, cavity acoustic evaluation, stability and control parameter estimation, air data calibration, and external flow evaluation.

Cavity acoustics were evaluated using measured pressure data. Of primary interest were sound pressure levels and frequency response curves. Analysis tools were primarily written for MATLAB. Several tools were developed to allow rapid analysis of acoustic data, giving engineers the ability to calculate and examine results from acoustic sensors in and around the telescope cavity. A batch analysis capability was created so that analysts could process data from an entire flight with one command.

Significant effort was put into completing the evaluation of the aerodynamic characteristics of the modified 747SP airplane in closed-door and open-door configurations. Parameter identification maneuvers were designed and then performed during closed and open door flight tests. Parameter estimation data analysis techniques were used in conjunction with existing aerodynamic models to create aerodynamic models for various airplane configu-

rations. Any differences between configurations were examined.

Air data calibration maneuvers were also flown and calibrations were developed for the various air data systems, including the airplane pitot static system and a Flush Air Data Sensing (FADS) system. Results were compared for different door configurations, to determine if door position affected air data measurements.

Qualitative airflow data were obtained during the closed- and open-

door flights using tufts on the aft portion of the fuselage. Video was taken from a chase plane. This video was analyzed for various flight conditions, and general flow descriptions of the aft fuselage of the 747SP were developed for the different closed and open door configurations.

This work was done by Stephen Cumming, Mike Frederick, and Mark Smith of Dryden Flight Research Center. For further information, contact Yvonne D. Gibbs at yvonne.d.gibbs@nasa.gov. DRC-010-016



Photo of 747SP SOFIA Airplane undergoing tests in an open-door configuration.

Sonic Thermometer for High-Altitude Balloons

A stand-alone version of the sensor would have utility as a gas composition sensor in industrial process situations.

Goddard Space Flight Center, Greenbelt, Maryland

The sonic thermometer is a specialized application of well-known sonic anemometer technology. Adaptations have been made to the circuit, including the addition of supporting sensors, which enable its use in the high-altitude environment and in non-air gas mixtures.

There is a need to measure gas temperatures inside and outside of super-pressure balloons that are flown at high altitudes. These measurements will allow the performance of the balloon to be modeled more accurately, leading to better flight performance. Small thermistors (solid-state temperature sensors) have been used for this general purpose, and for temperature measurements on radiosondes. A disadvantage to thermistors and other physical (as distinct from sonic) temperature sensors is that they are subject to solar heating errors when they are exposed to the Sun, and this leads to issues with their use in a very high-altitude environment.

While sonic anemometers and thermometers are commonly encountered

in surface-based applications, they are not found in a high-altitude [e.g., 100,000 ft (≈ 30.5 km) and above] environment. One reason for this is the very thin air and correspondingly poor sound propagation encountered at these altitudes. A second issue is that the gas temperature inside the balloon is required. Aside from mounting considerations, this also leads to a need to operate correctly in a helium or helium/air gas mixture. The gas composition must be known via some means in order to compute accurate temperatures.

To make accurate sonic temperature measurements, the mean molecular weight of the gas the sensor is working in must be known, as must the value for gamma (the ratio of gas heat capacity at constant pressure divided by gas heat capacity at constant volume) for that gas. Therefore, a supporting measurement is required that directly or indirectly allows gas composition and gamma to be determined. With this data, the speed of sound as measured by the sonic thermometer can then be used to compute an accurate temperature.

The key addition to the basic sonic thermometer design was a sensor that, in this case, measured gas heat capacity at constant pressure. This data could then be used to identify the gas mixture composition (ranging from pure helium to pure air), and with that data both mean gas molecular weight and gamma could be computed. In turn, this data is required for the temperature calculation.

The supporting sensor used for gas composition/molecular weight/gamma measurement is built as an integral part of the sonic thermometer circuitry, and consists of a pair of simple semiconductor sensors. During measurements, a gas composition measurement is made at the same time as a speed of sound measurement is made by the sonic thermometer. Thus, each measurement has its own gas composition data associated with it, enabling a precise temperature computation to be completed.

This work was done by John Bognar of Anasphere for Goddard Space Flight Center. Further information is contained in a TSP (see page 1). GSC-16104-1

Near-Infrared Photon-Counting Camera for High-Sensitivity Observations

Extremely faint phenomena and NIR signals emitted from distant celestial objects can be observed and imaged.

Goddard Space Flight Center, Greenbelt, Maryland

The dark current of a transferred-electron photocathode with an InGaAs absorber, responsive over the 0.9- to 1.7- μm range, must be reduced to an ultralow level suitable for low signal spectral astrophysical measurements by lowering the temperature of the sensor incorporating the cathode. However, photocathode quantum efficiency (QE) is known to reduce to zero at such low temperatures. Moreover, it has not been demonstrated that the target dark current can be reached at any temperature using existing photocathodes.

Changes in the transferred-electron photocathode epistructure (with an InGaAs absorber lattice-matched to InP

and exhibiting responsivity over the 0.9- to 1.7- μm range) and fabrication processes were developed and implemented that resulted in a demonstrated $>13\times$ reduction in dark current at -40°C while retaining $>95\%$ of the $\approx 25\%$ saturated room-temperature QE. Further testing at lower temperature is needed to confirm a $>25^\circ\text{C}$ predicted reduction in cooling required to achieve an ultralow dark-current target suitable for faint spectral astronomical observations that are not otherwise possible. This reduction in dark current makes it possible to increase the integration time of the imaging sensor, thus enabling a much higher near-infrared (NIR) sensitivity

than is possible with current technology. As a result, extremely faint phenomena and NIR signals emitted from distant celestial objects can be now observed and imaged (such as the dynamics of red-shifting galaxies, and spectral measurements on extra-solar planets in search of water and bio-markers) that were not previously possible. In addition, the enhanced NIR sensitivity also directly benefits other NIR imaging applications, including drug and bomb detection, stand-off detection of improvised explosive devices (IED's), Raman spectroscopy and microscopy for life/physical science applications, and semiconductor product defect detection.

A set of methods was developed for implementing an InGaAs photocathode whereby the dark current can be reduced by lowering the temperature to the ultralow target level, while at the same time, exhibiting QE that is high enough to perform the astrophysical measurements.

This innovation features a thin, n-type InP cap layer that is etched during final cleaning between the grid lines. Along with an n-type InP layer at the heterointerface and a p-type InP emitting surface layer, the extra degree-of-freedom provided by the n-type InP cap layer enables independent tailoring of the electric field at 3 key locations in the device: beneath the grid lines, at the emitting InP

surface between grid lines, and at the p-type InGaAs absorber/n-type InP heterointerface. This enables minimization of the field beneath the grid lines while the emitting surface and heterointerface fields are balanced such that the onset of high escape probability and turn-on completion of the heterointerface occur at the same reduced device bias. The resulting effect is that dark current components are minimized, including those due to undue extension of the depletion region into the low bandgap absorber and premature emitting surface field development with bias, while maintaining high QE and minimal grid line leakage.

The innovation features an InP:Zn emitting surface layer doped below the

onset of Zn diffusion (thus minimizing epitaxy and process variability), absence of an undoped InP drift layer (along with the avalanche-current-inducing voltage drop across it), and an InGaAs step grade layer introduced at the InGaAs absorber/InP:Si layer heterointerface (further reducing dark current components associated with the depleted low bandgap absorber). Employment of a SiON dielectric beneath the grid line promotes device stability and the absence of fixed mobile charge in the metal/dielectric/InP stack.

This work was done by Michael Jurkovic of Intevac Photonics for Goddard Space Flight Center. Further information is contained in a TSP (see page 1). GSC-16044-1

Integrated Optics Achromatic Nuller for Stellar Interferometry

Nuller allows faint off-axis light to be much more easily seen.

NASA's Jet Propulsion Laboratory, Pasadena, California

This innovation will replace a beam combiner, a phase shifter, and a mode conditioner, thus simplifying the system design and alignment, and saving weight and space in future missions. This nuller is a dielectric-waveguide-based, four-port asymmetric coupler. Its nulling performance is based on the mode-sorting property of adiabatic asymmetric couplers that are intrinsically achromatic. This nuller has been designed, and its performance modeled, in the 6.5-micrometer to 9.25-micrometer spectral interval (36% bandwidth). The calculated suppression of starlight for this 15-cm-long device is 10^{-5} or better through the whole bandwidth. This is enough to satisfy require-

ments of a flagship exoplanet-characterization mission.

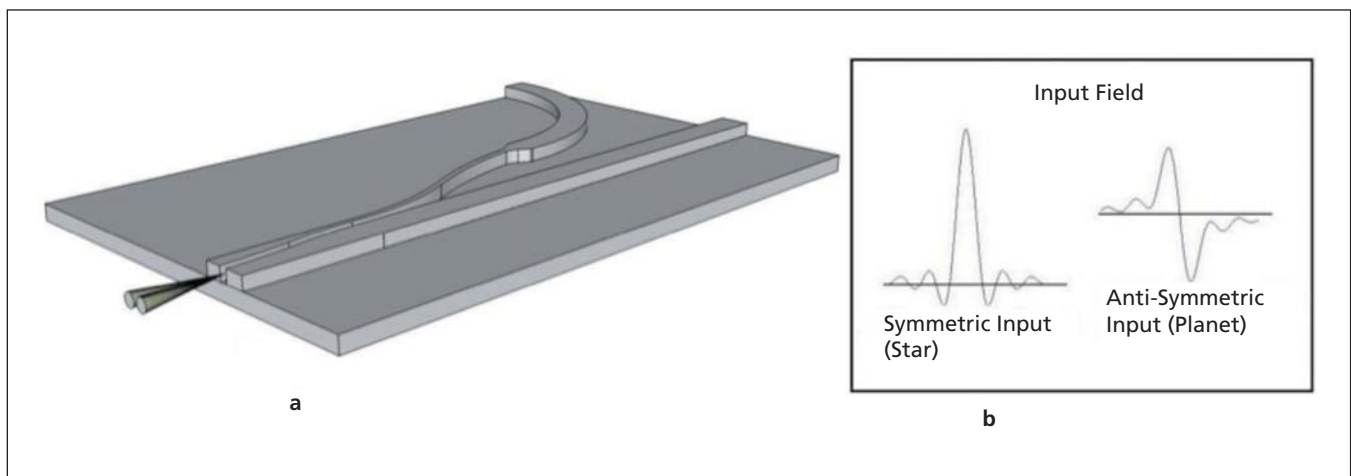
Nulling interferometry is an approach to starlight suppression that will allow the detection and spectral characterization of Earth-like exoplanets. Nulling interferometers separate the light originating from a dim planet from the bright starlight by placing the star at the bottom of a deep, destructive interference fringe, where the starlight is effectively cancelled, or nulled, thus allowing the faint off-axis light to be much more easily seen. This process is referred to as nulling of the starlight.

Achromatic nulling technology is a critical component that provides the

starlight suppression in interferometer-based observatories. Previously considered space-based interferometers are aimed at approximately 6-to-20-micrometer spectral range. While containing the spectral features of many gases that are considered to be signatures of life, it also offers better planet-to-star brightness ratio than shorter wavelengths.

In the Integrated Optics Achromatic Nuller (IOAN) device, the two beams from the interferometer's collecting telescopes pass through the same focusing optic and are incident on the input of the nuller.

The dual-input waveguide structure accommodates two modes, while each of



A 3-dimensional view of the **Integrated Optics Achromatic Nuller** device. (a) The scales are distorted for visual clarity. The input from the two telescopes is incident on the device from the left. (b) The input field for the case of the two telescope beams arriving in-phase (starlight) and exactly out-of-phase (planet light).

the output waveguides accommodates one mode only. At the input, the waveguide structure is symmetric and, therefore, the fundamental mode of the structure at the input is symmetric and the other mode is anti-symmetric. At the output, one of the waveguides is wider than the other, and therefore has a

higher effective refractive index. For the light originating from the star, if the interferometer is perfectly balanced, the input field in the focal plane of the focusing optic at the input of the device is symmetric, while for the light field originating from the planet (assuming the exact π phase shift) it is anti-symmetric.

Thus, in the two-mode input waveguide the starlight excites the fundamental mode, while the planet light excites the second, anti-symmetric, mode.

This work was done by Alexander Ksendzov of Caltech for NASA's Jet Propulsion Laboratory. Further information is contained in a TSP (see page 1). NPO-47834

High-Speed Digital Interferometry

Optical decoding eliminates the need for high-speed detectors and digital signal processing.

NASA's Jet Propulsion Laboratory, Pasadena, California

Digitally enhanced heterodyne interferometry (DI) is a laser metrology technique employing pseudo-random noise (PRN) codes phase-modulated onto an optical carrier. Combined with heterodyne interferometry, the PRN code is used to select individual signals, returning the inherent interferometric sensitivity determined by the optical wavelength. The signal isolation arises from the autocorrelation properties of the PRN code, enabling both rejection of spurious signals (e.g., from scattered light) and multiplexing capability using a single metrology system. The minimum separation of optical components is determined by the wavelength of the PRN code.

A variation of DI has 100 times reduction in the minimum component separation, allowing measurements of optical components only a few centimeters apart. Instead of the usual electronic decoding, the DI signal is interfered with an appropriately delayed, identically PRN-encoded, local oscillator beam. Optical decoding allows the use of a low-bandwidth signal processing chain with GHz codes,

negating the need for high-speed detectors and digital signal processing. This reduced bandwidth also reduces the power consumption of the entire system.

The heterodyne signal is created by off-set phase-locking two lasers with a digital phase-locked loop. The error-point is monitored on a dedicated phase-locking photoreceiver. PRN codes are phase-modulated by waveguide modulators onto each laser beam. These are subsequently interfered via a fiber beam-splitter, thus optically demodulating the laser signals, before being detected on a signal photoreceiver. One PRN code is digitally delayed with respect to the other in order to align the codes with respect to the reflected light from an optic under interrogation, thus optically demodulating the signal for that specific mirror. The delay is altered (controlled digitally) to pick out any one of the optics under interrogation.

At the time of this reporting, this is the first known time that DI has been employed to measure optics separated by less than meters, down to a few centimeters. This was achieved by implementing,

for the first time, optical demodulation of the encoded laser beams (as opposed to the more traditional/common electronic demodulation). This technique is entirely implemented in software via hardware that would already exist onboard a spacecraft. This reduces complexity, power consumption, volume, and risk of failure.

There are many proposed missions that will employ lasers and require extremely high-resolution metrology. Digital interferometry can be implemented and achieve sub-10-pm resolution. With this new technique, the metrology can be performed on optical components separated by centimeters. This allows measurements of optics on a single optical bench within a single spacecraft, in addition to inter-spacecraft metrology measurements.

This work was done by Glenn De Vine, Daniel A. Shaddock, Brent Ware, Robert E. Spero, Danielle M. Wuchenich, William M. Klipstein, and Kirk McKenzie of Caltech for NASA's Jet Propulsion Laboratory. Further information is contained in a TSP (see page 1). NPO-47886

Ultra-Miniature Lidar Scanner for Launch Range Data Collection

New scanning technology promises at least a 10× performance improvement.

John F. Kennedy Space Center, Florida

The most critical component in lidar is its laser scanner, which delivers pulsed or CW laser to target with desirable field of view (FOV). Most existing lidars use a rotating or oscillating mirror for scanning, resulting in several drawbacks.

A lidar scanning technology was developed that could achieve very high scan-

ning speed, with an ultra-miniature size and much lighter weight. This technology promises at least a 10× performance improvement in these areas over existing lidar scanners. Features of the proposed ultra-miniature lidar scanner include the ability to make the entire scanner <2 mm in diameter; very high scanning speed

(e.g. 5–20 kHz, in contrast to several hundred Hz in existing scanners); structure design to meet stringent requirements on size, weight, power, and compactness for various applications; and the scanning speed and FOV can be altered for obtaining high image resolutions of targeted areas and for diversified uses.

This technology employs a single-mode optical fiber attached to the end of a mini tube made of piezoelectric material. The two-degrees-of-freedom (DOF) piezo tube is driven at the first mode of mechanical resonance frequency of the fixed-free cantilevered fiber. The gain of mechanical resonance allows a small vibration at the tip of the piezo tube to be amplified several hundred times to vibrate the tip of the optical fiber. The laser beam is delivered through the single-mode fiber and the vibrating fiber at high resonance frequency (e.g., 5–20 kHz), and generates scanning patterns with desirable FOV.

A laser beam is delivered via the single fiber core to the target surface. The direction of the light beam delivered by

the single fiber is controlled by two piezoelectric drivers mounted orthogonally on the mounting base of the single fiber to generate a controllable motion of the cantilevered fiber with two degrees of freedom. With proper optics, the directed light beam produces a bright spot on the object surface. The reflected light energy from this spot is collected by multiple optical fibers embedded into the outer housing. These light collectors form a “fiber ring.” The time duration between the beginning of the laser pulse and receiving pulse (in the case of pulse laser) or phase difference between emitted and received signals (in the case of CW laser) determines the target distance, based on time-of-flight principle.

The single-fiber core moves in an area-fill fashion to produce laser light spot sequentially over a target surface, and light collectors record the timing and brightness of these data points in a pixel-by-pixel fashion. The signal receiver, piezo controller, and the laser source are all connected to the distal end via flexible fiber/wire bundle with diameter less than one millimeter. A control computer is used to control the piezo driver motion, laser timing and intensity, returned signal processing, and 3D data construction and visualization.

This work was done by Jason Geng of Xigen LLC under the Small Business Innovation Research Program for Kennedy Space Center. Further information is contained in a TSP (see page 1). KSC-13570



Shape and Color Features for Object Recognition Search

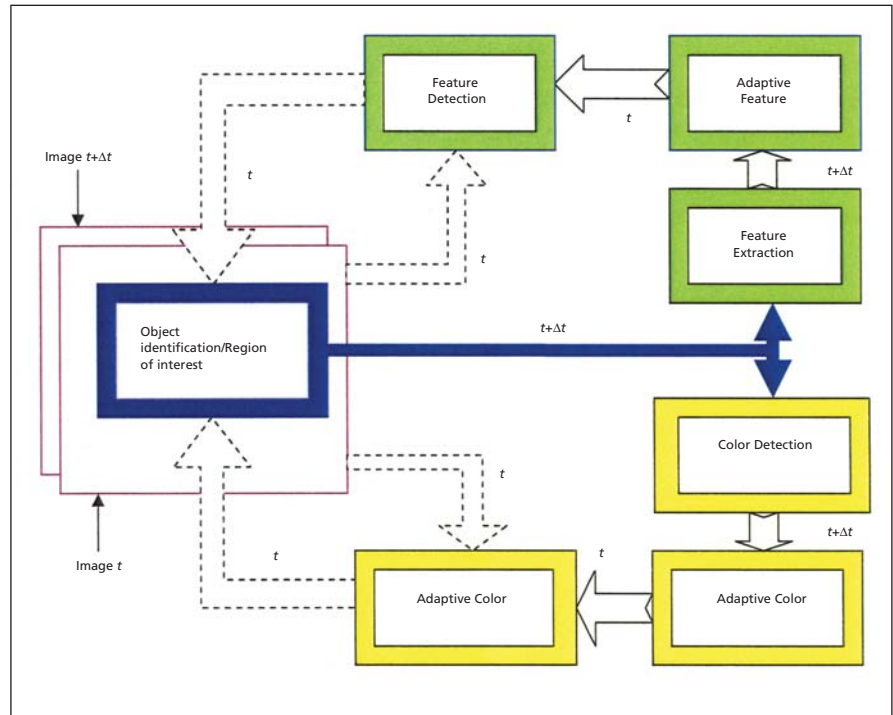
This technique can be used in Internet image searching, intelligent video, and security and surveillance applications.

NASA's Jet Propulsion Laboratory, Pasadena, California

A bio-inspired shape feature of an object of interest emulates the integration of the saccadic eye movement and horizontal layer in vertebrate retina for object recognition search where a single object can be used one at a time. The optimal computational model for shape-extraction-based principal component analysis (PCA) was also developed to reduce processing time and enable the real-time adaptive system capability. A color feature of the object is employed as color segmentation to empower the shape feature recognition to solve the object recognition in the heterogeneous environment where a single technique — shape or color — may expose its difficulties. To enable the effective system, an adaptive architecture and autonomous mechanism were developed to recognize and adapt the shape and color feature of the moving object.

The bio-inspired object recognition based on bio-inspired shape and color can be effective to recognize a person of interest in the heterogeneous environment where the single technique exposed its difficulties to perform effective recognition. Moreover, this work also demonstrates the mechanism and architecture of the autonomous adaptive system to enable the realistic system for the practical use in the future.

This work was done by Tuan A. Duong and Vu A. Duong of Caltech, and Allen R. Stubberud of UCI for NASA's Jet Propulsion



The Color and Shape Feature Feedback Adaptive architecture.

Laboratory. For more information, contact iaoffice@jpl.nasa.gov.

In accordance with Public Law 96-517, the contractor has elected to retain title to this invention. Inquiries concerning rights for its commercial use should be addressed to:

Innovative Technology Assets Management
JPL

Mail Stop 202-233

4800 Oak Grove Drive

Pasadena, CA 91109-8099

E-mail: iaoffice@jpl.nasa.gov

Refer to NPO-47065, volume and number of this NASA Tech Briefs issue, and the page number.

Explanation Capabilities for Behavior-Based Robot Control

This mathematical framework can be applied to search and rescue or remote exploration robotic systems.

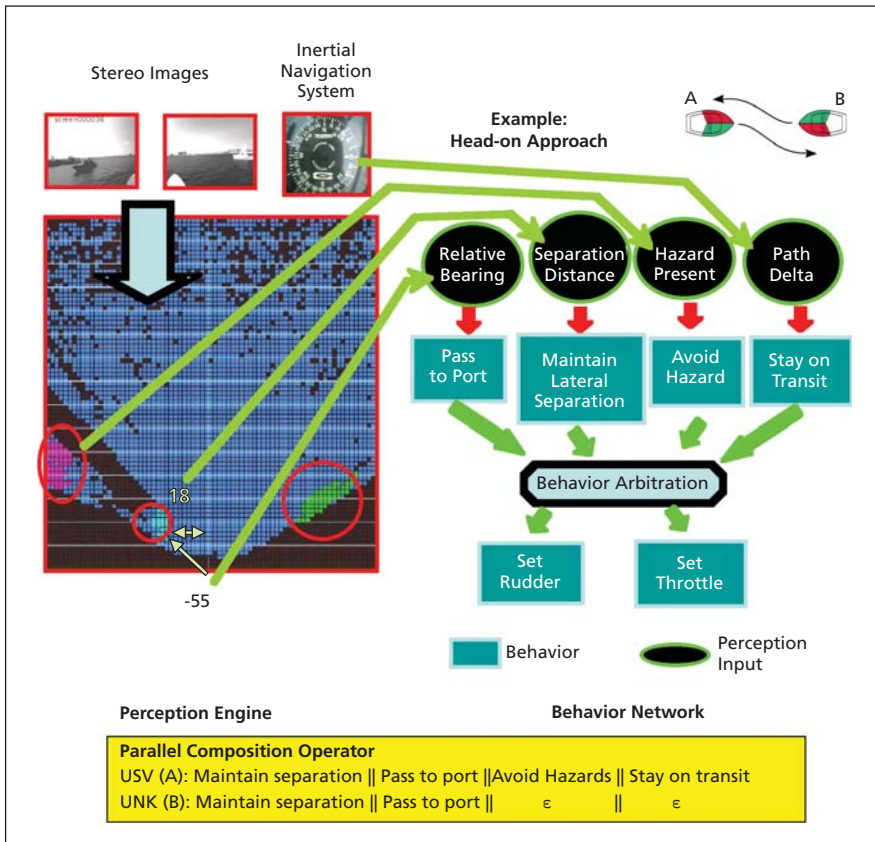
NASA's Jet Propulsion Laboratory, Pasadena, California

A recent study that evaluated issues associated with remote interaction with an autonomous vehicle within the framework of grounding found that missing contextual information led to uncertainty in the interpretation of collected data,

and so introduced errors into the command logic of the vehicle. As the vehicles became more autonomous through the activation of additional capabilities, more errors were made. This is an inefficient use of the platform, since the behavior of

remotely located autonomous vehicles didn't coincide with the "mental models" of human operators.

One of the conclusions of the study was that there should be a way for the autonomous vehicles to describe what



An example of the **Inference Mechanism** in a Rules-of-the-Road behavior shows two boats approaching each other head-on. The left side shows the sensory inputs that are needed by the behaviors that are competing with each other to control the actuators. The right side shows the behavior network with four behaviors fed into the Arbitration module to produce the settings for the rudder (heading) and throttle (speed) of the vehicle. Mapping of the behavior network to an equivalent cost-calculus expression is shown at the bottom.

action they choose and why. Robotic agents with enough self-awareness to dynamically adjust the information conveyed back to the Operations Center based on a detail level component analysis of requests could provide this description capability. One way to accomplish

this is to map the behavior base of the robot into a formal mathematical framework called a cost-calculus. A cost-calculus uses composition operators to build up sequences of behaviors that can then be compared to what is observed using well-known inference mechanisms.

The explanation system is broken up into three subsystems that address the principal developments needed:

1. An inference mechanism for the mapping of observed behaviors into the cost-calculus: The observation equivalence of behaviors on a single autonomous agent and between two or more agents is done through bi-simulation relations. An example of the inference mechanism at work in a Rules-of-the-Road behavior is shown in the figure.
2. A learning mechanism for the cost-expression generation for observed behaviors outside of the cost-calculus tactical behavior base: Reinforcement learning of observed behavior patterns is used for the common grounding of behaviors sequences that were not previously observed, or that are in the command dictionary of the autonomous agent.
3. Explanation capabilities for the system: A dynamic decision tree decomposition of the observed behaviors is used to generate a set of rules for explanation. An adaptive level of detail is automatically built into this process in that all of the sensory information that led to a behavior is available, and can be conveyed to the operator if the human/machine interface (HMI) has a detail level of request capability.

This work was done by Terrance L. Huntsberger of Caltech for NASA's Jet Propulsion Laboratory. Further information is contained in a TSP (see page 1).

The software used in this innovation is available for commercial licensing. Please contact Daniel Broderick of the California Institute of Technology at danielb@caltech.edu. Refer to NPO-46864.

➤ A DNA-Inspired Encryption Methodology for Secure, Mobile Ad Hoc Networks

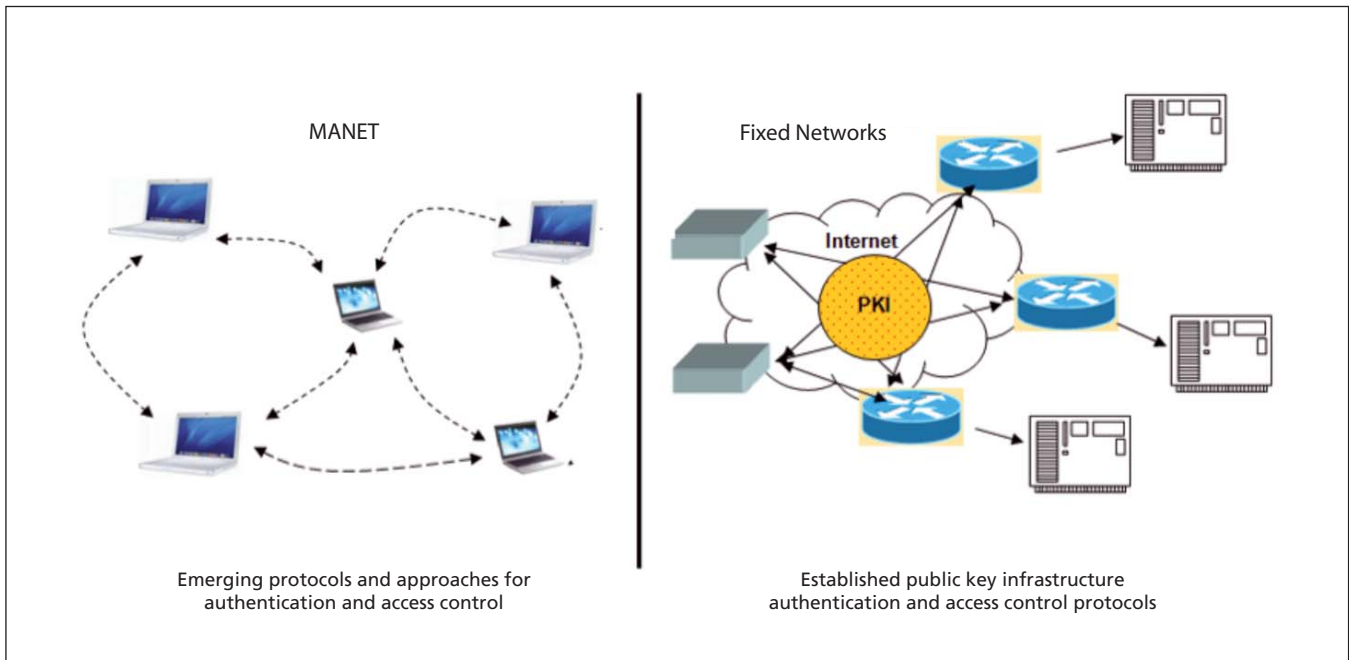
An encryption mechanism uses the principles of DNA replication and steganography.

Goddard Space Flight Center, Greenbelt, Maryland

Users are pushing for greater physical mobility with their network and Internet access. Mobile *ad hoc* networks (MANET) can provide an efficient mobile network architecture, but security is a key concern. The figure summarizes differences in the state of network security for MANET and fixed networks. MANETs require the ability to distinguish trusted peers, and tolerate the

ingress/egress of nodes on an unscheduled basis. Because the networks by their very nature are mobile and self-organizing, use of a Public Key Infrastructure (PKI), X.509 certificates, RSA, and nonce exchanges becomes problematic if the ideal of MANET is to be achieved. Molecular biology models such as DNA evolution can provide a basis for a proprietary security architecture that

achieves high degrees of diffusion and confusion, and resistance to cryptanalysis. A proprietary encryption mechanism was developed that uses the principles of DNA replication and steganography (hidden word cryptography) for confidentiality and authentication. The foundation of the approach includes organization of coded words and messages using base pairs organized into genes,



MANET versus fixed network security.

an expandable genome consisting of DNA-based chromosome keys, and a DNA-based message encoding, replication, and evolution and fitness. In evolutionary biology, fitness is a characteristic that relates to the number of offspring produced from a given genome. From a population genetics point of view, the relative fitness of the mutant depends upon the number of descendants per wild-type descendant. In evolutionary computing, a fitness algorithm determines whether candidate solutions, in this case encrypted messages, are sufficiently encrypted to be transmitted.

The technology provides a mechanism for confidential electronic traffic over a MANET without a PKI for authenticating users. Users may enter and leave a network at will. Users may alternate between trusted, untrusted, unknown, and mali-

cious behavior. Existing mobile networks rely on PKI-provided certificates and public encryption standards such as AES (Advanced Encryption Standard). These are public standards, subject to continuous scrutiny for methods of attacking the underlying basis of security.

The DNA-inspired approach uses a rapidly evolving genome to resist cryptographic analyses. It produces one-way (encryption only) and two-way (encryption/decryption) codes. Because of the dynamic, evolutionary nature of this approach, potential intruders must continually intercept decoding instructions between source and destination. Missing one generation of genome decryption information seriously corrupts the decryption process. Missing multiple generations eventually renders previous decryption analyses useless. Potential at-

tackers are likely to be unable to continuously intercept all traffic. The genome becomes more fit relative to cryptographic analyses. Furthermore, DNA provides a convenient molecule to establish a new type of physical layer encryption through which encryption codes are instantiated through biochemical means and read back or modified by biochemical means. Such encryption models provide “Security by Obscurity.”

Areas of interest include proprietary secure virtual private MANETs, military MANETs, mobile-commercial MANETs, covert surveillance and tracking of goods, and commercial surveillance and tracking of goods.

This work was done by Harry Shaw of Goddard Space Flight Center. Further information is contained in a TSP (see page 1). GSC-15374-1



Quality Control Method for a Micro-Nano-Channel Microfabricated Device

This method can be performed on multiple devices simultaneously or one at a time as quality control.

Lyndon B. Johnson Space Center, Houston, Texas

A variety of silicon-fabricated devices is used in medical applications such as drug and cell delivery, and DNA and protein separation and analysis. In applications such as drug delivery from implantable devices, the silicon device structure must have superior precision. In particular, the nano-channel size in implantable drug delivery membranes strongly determines the drug release from the implanted reservoir. An accidental difference in the nano size may translate into ineffective medical treatment or dangerous overdosing.

When a fluidic device inlet is connected to a compressed gas reservoir, and the outlet is at a lower pressure, a gas flow occurs through the membrane toward the outside. The method relies on the measurement of the gas pressure over the elapsed time inside the upstream and downstream environments. By knowing the volume of the upstream reservoir, the gas flow rate through the membrane over the pressure drop can be calculated.

This quality control method consists of measuring the gas flow through a de-

vice and comparing the results with a standard curve, which can be obtained by testing standard devices. Standard devices can be selected through a variety of techniques, both destructive and non-destructive, such as SEM, AFM, and standard particle filtration.

In this innovation, the method can be performed on multiple devices at once or one at a time as quality control for large-scale production. The testing device can be designed to perform the measurement testing in less than one minute. The testing gas can be chosen to not change or affect the surface properties of the devices, making it a non-destructive method. Also, the method can be performed during the production process, even inside a cleanroom on wafers or on final products as a conformity test. The testing system does not require expensive instruments, can be designed as a portable device, can be automated, and is flexible enough to be used on a variety of devices.

The system accuracy depends on the pressure sensor used. Commercially

available pressure sensors allow building extremely high accuracy testing systems with high sensitivity and high reproducibility. Additionally, the system does not require specific expertise to be used.

This work was done by Alessandro Grattoni, Mauro Ferrari, and Xuewu Li of the University of Texas Health Science Center for Johnson Space Center. For further information, contact the Johnson Technology Transfer Office at (281) 483-3809.

In accordance with Public Law 96-517, the contractor has elected to retain title to this invention. Inquiries concerning rights for its commercial use should be addressed to:

*Office of Technology Management
The University of Texas Health Science
Center at Houston
7000 Fannin Street, Suite 720
Houston, TX 77030
Phone No.: (713) 500-3383*

E-Mail: christine.flynn@uth.tmc.edu

Refer to MSC-24489-1, volume and number of this Medical Design Briefs issue, and the page number.



Books & Reports

Corner-Cube Retroreflector Instrument for Advanced Lunar Laser Ranging

A paper describes how, based on a structural-thermal-optical-performance analysis, it has been determined that a single, large, hollow corner cube (170-mm outer diameter) with custom dihedral angles offers a return signal comparable to the Apollo 11 and 14 solid-corner-cube arrays (each consisting of 100 small, solid corner cubes), with negligible pulse spread and much lower mass. The design of the corner cube, and its surrounding mounting and casing, is driven by the thermal environment on the lunar surface, which is subject to significant temperature variations (in the range between 70 and 390 K). Therefore, the corner cube is enclosed in an insulated container open at one end; a narrow-band-pass solar filter is used to reduce the solar energy that enters the open end during the lunar day, achieving a nearly uniform temperature inside the container. Also, the materials and adhesive techniques that will be used for this corner-cube reflector must have appropriate thermal and mechanical characteristics (e.g., silica or beryllium for the cube and aluminum for the casing) to further reduce the impact of the thermal environment on the instrument's performance.

The instrument would consist of a single, open corner cube protected by a separate solar filter, and mounted in a cylindrical or spherical case. A major goal in the design of a new lunar ranging system is a measurement accuracy improvement to better than 1 mm by reducing the pulse spread due to orientation. While achieving this goal, it was desired to keep the intensity of the return beam at least as bright as the Apollo 100-corner-cube arrays. These goals are met in this design by increasing the optical aperture of a single corner cube to approximately 170 mm outer diameter. This use of an "open" corner cube allows the selection of corner cube materials to be based primarily on thermal considerations, with no requirements on optical transparency. Such a corner cube also allows for easier pointing requirements, because there is no dependence on total internal reflection, which can fail off-axis.

This work was done by Slava G. Turyshev, William M. Folkner, Gary M. Gutt, James G. Williams, Ruwan P. Somawardhana, and Richard T. Baran of Caltech for NASA's Jet Propulsion Laboratory. Further information is contained in a TSP (see page 1). NPO-47489

Electrospray Collection of Lunar Dust

A report describes ElectroSpray Ionization based Electrostatic Precipitation (ESIEP) for collecting lunar dust particles. While some HEPA filtration processes may remove a higher fraction (>99.9 percent) of the particles, the high efficiency may not be appropriate from an overall system standpoint, especially in light of the relatively large power requirement that such systems demand.

The new electrospray particle capture technology (inspired by the late Nobel Laureate Dr. John B. Fenn) is described as a variant of electrostatic precipitation that eliminates the current drawbacks of electrostatic precipitation. The new approach replaces corona prone field with a mist of highly charged micro-droplets generated by electrospray ionization (ESI) as the mechanism by which incoming particles are attracted and captured. In electrospray, a minuscule flow rate (microliters/minute) of liquid (typically water and a small amount of salt to enhance conductivity) is fed from the tip of a needle held at a high voltage potential relative to an opposite counter electrode. At sufficient field strength, a sharp liquid meniscus forms (known as a so-called "Taylor Cone"), which emits a jet of highly charged droplets that drift through the surrounding gas and are collected on the walls of a conductive tube. Particles in the gas have a high probability of contact with the droplets either by adhering to the droplets or otherwise acquiring a high level of charge, causing them to be captured on the collecting electrode as well. The spray acts as a filtration material that is continuously introduced and removed from the gas flow, and thus can never become clogged.

Experiments determined that ESIEP can collect particles with efficiencies as high as or higher than traditional corona-based EP, owing to the higher specificity of charging and higher levels

of charge deposited on particles by the droplets. Removal rates of 95–99 percent and greater are typically observed, even at moderate gas flow rates — all without the generation of ozone due to corona discharge.

This work was done by Joseph Bango and Michael Dziekan of Connecticut Analytical Corp. for Glenn Research Center. Further information is contained in a TSP (see page 1).

Inquiries concerning rights for the commercial use of this invention should be addressed to NASA Glenn Research Center, Innovative Partnerships Office, Attn: Steven Fedor, Mail Stop 4–8, 21000 Brookpark Road, Cleveland, Ohio 44135. Refer to LEW-18629-1.

Fabrication of a Kilopixel Array of Superconducting Microcalorimeters With Microstripline Wiring

A document describes the fabrication of a two-dimensional microcalorimeter array that uses microstrip wiring and integrated heat sinking to enable use of high-performance pixel designs at kilopixel scales (32×32). Each pixel is the high-resolution design employed in small-array test devices, which consist of a Mo/Au TES (transition edge sensor) on a silicon nitride membrane and an electroplated Bi/Au absorber. The pixel pitch within the array is 300 microns, where absorbers 290 microns on a side are cantilevered over a silicon support grid with 100-micron-wide beams. The high-density wiring and heat sinking are both carried by the silicon beams to the edge of the array. All pixels are wired out to the array edge.

ECR (electron cyclotron resonance) oxide underlayer is deposited underneath the sensor layer. The sensor (TES) layer consists of a superconducting underlayer and a normal metal top layer. If the sensor is deposited at high temperature, the ECR oxide can be vacuum annealed to improve film smoothness and etch characteristics.

This process is designed to recover high-resolution, single-pixel x-ray microcalorimeter performance within arrays of arbitrarily large format. The critical current limiting parts of the circuit are designed to have simple interfaces that can be independently verified. The lead-to-TES interface is entirely de-

terminated in a single layer that has multiple points of interface to maximize critical current. The lead rails that overlap the TES sensor element contact both the superconducting underlayer and the TES normal metal.

This work was done by James Chervenak of Goddard Space Flight Center. Further information is contained in a TSP (see page 1). GSC-15915-1

Spacecraft Attitude Tracking and Maneuver Using Combined Magnetic Actuators

A paper describes attitude-control algorithms using the combination of magnetic actuators with reaction wheel assemblies (RWAs) or other types of actuators such as thrusters. The combination of magnetic actuators with one or two RWAs aligned with different body axis expands the two-dimensional control torque to three-dimensional. The algorithms can guarantee the spacecraft attitude and rates to track the commanded attitude precisely.

A design example is presented for nadir-pointing, pitch, and yaw maneuvers. The results show that precise attitude tracking can be reached and the attitude-control accuracy is comparable with RWA-based attitude control. When there are only one or two workable

RWAs due to RWA failures, the attitude-control system can switch to the control algorithms for the combined magnetic actuators with the RWAs without going to the safe mode, and the control accuracy can be maintained.

The attitude-control algorithms of the combined actuators are derived, which can guarantee the spacecraft attitude and rates to track the commanded values precisely. Results show that precise attitude tracking can be reached, and the attitude-control accuracy is comparable with 3-axis wheel control.

This work was done by Zhiqiang Zhou of Langley Research Center. Further information is contained in a TSP (see page 1). LAR-17862-1

Coherent Detector for Near-Angle Scattering and Polarization Characterization of Telescope Mirror Coatings

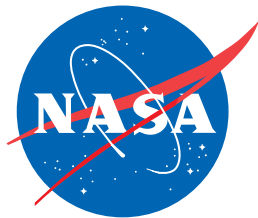
A report discusses the difficulty of measuring scattering properties of coated mirrors extremely close to the specular reflection peak. A prototype Optical Heterodyne Near-angle Scatterometer (OHNS) was developed. Light from a long-coherence-length (>150 m) 532-nm laser is split into two arms. Acousto-optic modulators frequency shift the sample and reference

beams, establishing a fixed beat frequency between the beams. The sample beam is directed at very high f/# onto a mirror sample, and the point spread function (PSF) formed after the mirror sample is scanned with a pinhole. This light is recombined by a non-polarizing beam splitter and measured through heterodyne detection with a spectrum analyzer. Polarizers control the illuminated and analyzed polarization states, allowing the polarization dependent scatter to be measured.

The bidirectional reflective or scattering distribution function is normally measured through use of a scattering goniometer instrument. The instrumental beam width (collection angle span) over which the scatterometer responds is typically many degrees. The OHNS enables measurement at angles as small as the first Airy disk diameter.

This work was done by Steven A. Macenka of Caltech and Russell A. Chipman, Brian J. Daugherty, and Stephen C. McClain of the University of Arizona for NASA's Jet Propulsion Laboratory. Further information is contained in a TSP (see page 1).

This invention is owned by NASA, and a patent application has been filed. Inquiries concerning nonexclusive or exclusive license for its commercial development should be addressed to the Patent Counsel, NASA Management Office-JPL. Refer to NPO-47310.



National Aeronautics and
Space Administration